UNITED NATIONS UNIVERSITY
GEOTHERMAL TRAINING PROGRAMME
Orkustofnun, Grensasvegur 9,
IS-108 Reykjavik, Iceland

Reports 2013
Number 32

INTERPRETATION OF RECENT TEMPERATURE AND PRESSURE DATA AND UPDATED CONCEPTUAL MODEL OF THE GREATER OLKARIA GEOTHERMAL SYSTEM, KENYA

Eric Rop
Kenya Electricity Generating Company, Ltd. – KenGen
Olkaria Geothermal Project
P.O. Box 785-20117, Naivasha,
KENYA
erop@kengen.co.ke

ABSTRACT

Optimal development and utilisation of geothermal resources is dependent on the understanding of their size and nature, both in the natural undisturbed state as well as the dynamic response as a result of utilisation, hence the need to develop a conceptual model.

The conceptual model is the main input for the complex field numerical modelling for resource estimates and field development plans. The temperature and pressure models are used as the basis for geothermal field concept development as well as geothermal well discharge characteristics such as enthalpy, mass flow and chemistry. The geology, geochemistry, geophysical information, surface geology and borehole geology play a significant role in understanding the heat source, the permeability, flow patterns and the origin of hot and cold recharge of a geothermal system.

The Olkaria Conceptual model has been updated several times, since the first simple one was presented by Sweco and Virkir in 1976, as new data was acquired. The present model was presented by the consortium of Mannvit/ÍSOR/Vatnaskil/Verkís during the field optimisation study in 2012.

This report presents the updated temperature and pressure model of the Greater Olkaria geothermal system, based on newly acquired temperature and pressure data through ongoing drilling operations in the field. The perceived change in the conceptual model of the field as result of this new data is also pointed out and recommendations made on further drilling sites to give a better understanding of the Olkaria geothermal resource.

1. INTRODUCTION

The Greater Olkaria geothermal field is a high temperature geothermal system located in the Kenya Rift Valley which is part of the tectonically active East African Rift valley, extending from the Afar triple junction at the Gulf of Eden in Mozambique, to the south. The Rift valley splits into the Western Rift system and the Eastern Rift system on entering the Eastern Africa region. Seventeen volcanic centres

have been identified in the Kenya Rift system and geothermal activity has been found associated with eleven of them. Figure 1 shows the location of the Greater Olkaria Geothermal field within the Kenya Rift valley.

The field is divided into sectors as shown in Figure 2. These sectors are: Olkaria East, Olkaria Northeast, Olkaria South West, Olkaria Central, Olkaria North West, Olkaria South East and the Olkaria Domes field. Three power plants are currently operating: Olkaria I and II, operated by KenGen, are generating a total of 155 MWe, including a 5 MWe well head unit pilot plant, while Olkaria III, operated by OrPower 4 Inc., is generating a total of 84 MWe. At present, power plants with a generating capacity of 280 MWe are under construction, utilising steam both from Olkaria East (Olkaria I) and Domes geothermal fields.

The wells in the North West part of the field are utilised by the Oserian farm for domestic power generation and direct heating of green houses. Spa facilities and heated swimming pools are also under construction to utilise the steam and hot water from Olkaria II power station for heating purposes.

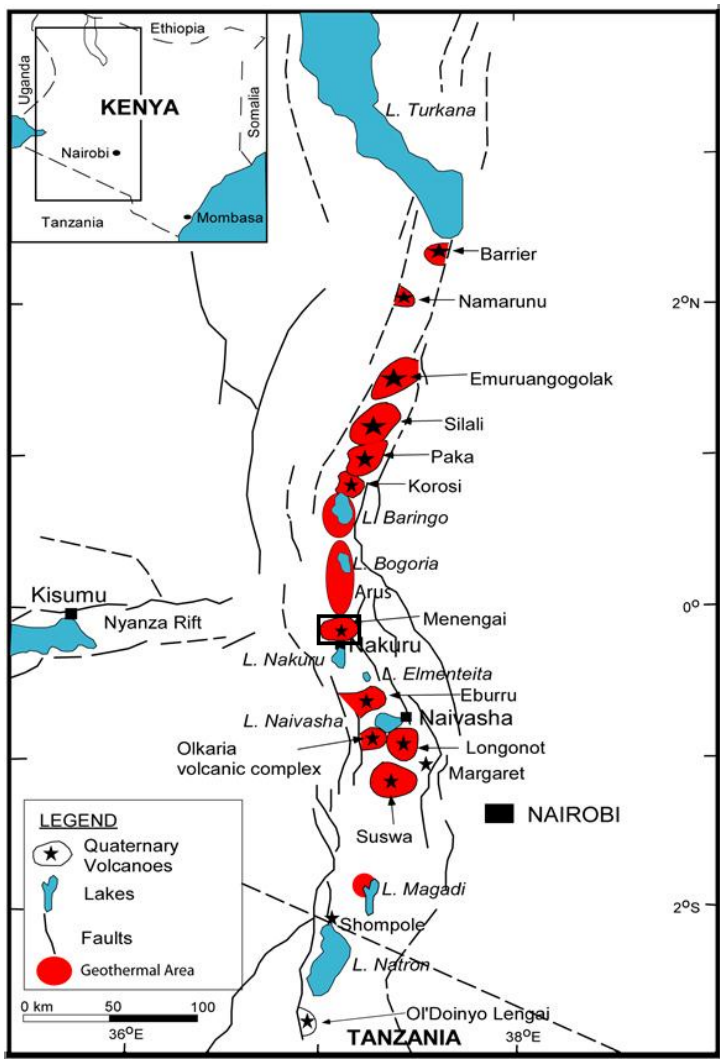

FIGURE 1: Map showing the Greater Olkaria Geothermal prospect within the Kenyan Rift Valley

The recent optimisation study, carried out in 2011 by the Mannvit/ÍSOR/Vatnaskil/Verkís consortium, divided the Olkaria geothermal resource into two parts:

1. The heavily explored part;
2. The periphery and less explored parts.

The *Heavily explored part* is defined as the part of the Olkaria field where good geophysical and reservoir information was available at the time of the study. Through extensive drilling and long term utilization data, the production response in this part of the field is well defined and understood. Hence, a more representative conceptual model was developed (Mannvit/ÍSOR/Vatnaskil/Verkís, 2011).

The electrical generating capacity of the heavily explored part of KenGen's concession area in Olkaria is estimated to be about 630 MWe based on volumetric resource assessment, lumped parameter pressure response modelling and detailed numerical modelling (Mannvit/ÍSOR/Vatnaskil/Verkís, 2012a and b). This includes the 150 MWe already installed and the 280 MWe currently in the final stages of power plant construction.

The less explored part, on the other hand, is explained as where drilling has been limited and mainly indirect indications of an exploitable resource exist. Therefore, the model for this part is deduced as being very speculative. The electrical generating capacity of the less explored part is estimated to be 300 MWe, based on a volumetric assessment (Mannvit/ÍSOR/ Vatnaskil/Verkís, 2012a). The consortium recommended that the anticipated resources in the less explored parts be further explored through comprehensive surveying and drilling.

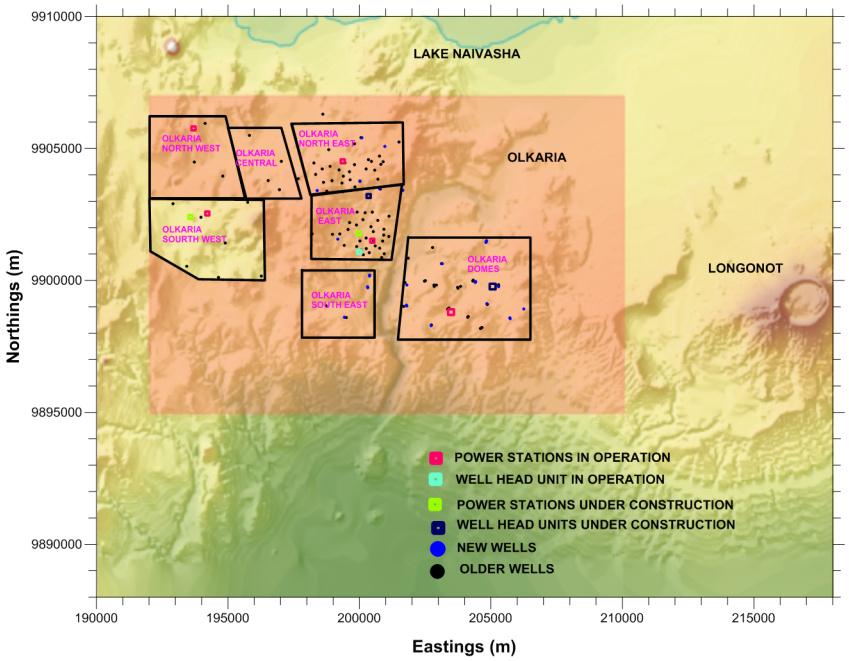

FIGURE 2: The Greater Olkaria geothermal field and subsectors

Upon recommendations of the present optimisation study, KenGen embarked on extensive drilling of more production wells in the heavily explored parts and step out drilling in the less explored parts in an effort to try and delineate the extent of the resource. As a result of this drilling, new data has been obtained which requires analysis and interpretation to aid in updating the present conceptual model of the less explored part, thus providing more understanding of the geothermal field. The new data was acquired quickly from present drilling operations which involved 8 drilling rigs. It is imperative that the data analysis and interpretation be kept at pace with the drilling operations so as to guide the operation and aid the management in making critical decisions regarding the optimised development of the field.

An effort is, therefore, made in this report to update the temperature and pressure models of the Greater Olkaria Geothermal field, critical input in calibrating the natural state geothermal reservoir model as well as for formulating a field development plan. An effort is also made to point out the effects of the newly acquired data on the present conceptual model.

2. THE GREATER OLKARIA GEOTHERMAL SYSTEM

The rift system has experienced repeated upwarping volcanism of mostly rhyolitic and trachytic rocks which started 20 million years ago. Upwelling of the asthenosphere provides the driving mechanism for the lithospheric uplift and extension (Clarke et al., 1990). Structures of the rift valley vary both perpendicularly and along the rift.

2.1 Geology

Olkaria geothermal system is believed to have been active from late Pleistocene to Holocene Age (Clarke et al., 1990). The geothermal field is inside a major volcanic complex cut by N-S normal rifting faults, trending NW-SE and WNW-ESE. It has numerous rhyolitic domes forming a ring structure associated with the major fractures and magmatic activity. The ring structure is more pronounced in the eastern and southeast parts of the Domes field. The ring structure breaks into outer and inner parts in the southeast part. The most prominent volcanic structures are the Ol'Njorowa gorge, N-S trending

Ololbutot fault, NE trending Olkaria fault, the Olkaria fracture, Suswa fault, and the Gorge Farm fault (Muchemi, 1999). Figure 3 below shows a geological map of the Olkaria volcanic system.

Eruptions associated with the Olkaria volcano and the Ololbutot fault zone have produced rhyolitic and obsidian flows. Much of the surface manifestations have been concealed by pyroclastic ash eruptions from the Longonot and Suswa volcanoes, making it difficult to predict the throws and offset of fractures from the surface. Several geothermal manifestations occur along these fractures and faults. The clustered ring structures may indicate several magma sources, but of the same geological age as evident from the surface (Mungania, 1999).

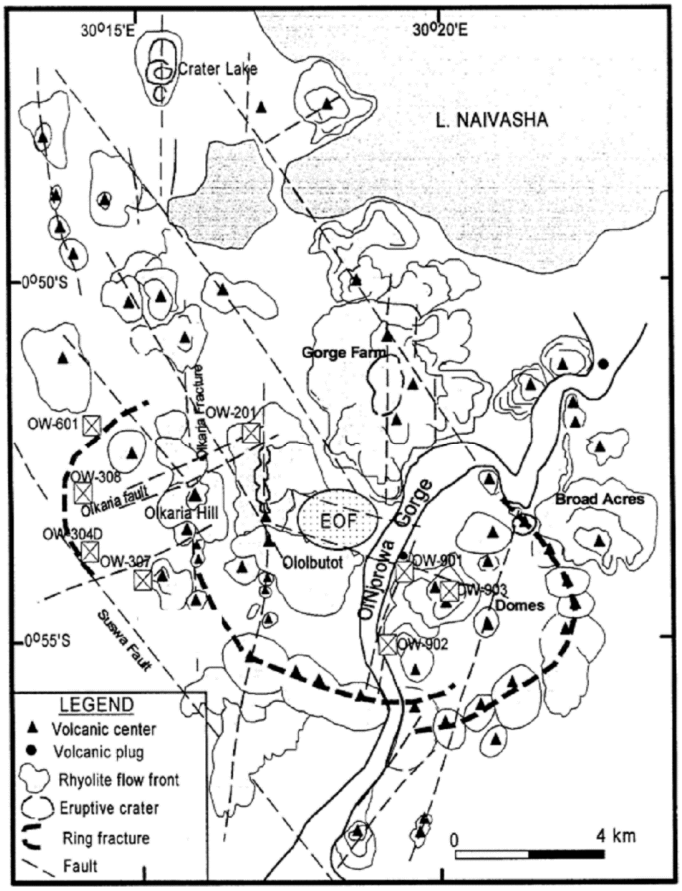

FIGURE 3: Map of the Greater Olkaria volcanic complex showing volcanism and tectonics (Muchemi, 1999)

Stratigraphic information indicates that the subsurface is dominated by rhyolitic tuffs and breccias with subordinate trachytes followed by a series of basaltic lavas of various thicknesses, intercalated with trachytes. These are followed by a thick series of trachytic lavas, subordinate basalt and acidic volcanic rocks which are replaced by the Mau tuffs in the western part of the field. Intrusions which are believed to be associated with permeability are rarely encountered in Olkaria wells, as the dipper stratigraphy is mainly dense trachytic lavas (Muchemi, 1999).

The basaltic series found in the Olkaria wells are excellent marker beds forming a sub-horizontal landscape for tectonic faults. The boundary between the rhyolitic pyroclastic succession and the underlying trachytes with the intercalating basalt series marks the onset of the Olkaria volcano (Mannvit/ÍSOR/Vatnaskil/Verkís, 2011). The level of basalt is observed to be similar between the tectonically quiet East field, but is more pronounced in the Domes field, inferring NE-SW faulting and may coincide with the proposed inner caldera fracture.

2.2 Geophysical survey

The gravity survey of the shallow crust beneath Olkaria shows a general gravity high tending north-northwest and in line with regional geological structures. However, there are local highs that trend northeast in line with recent fault trends. These local gravity highs are interpreted as dyke intrusions which are heat sources in some areas while in others, e.g. along the Ololbutot fault zone, they act as hydrological barriers between fields (Maarita, 2009).

Some earlier geological studies suggested the presence of a caldera at Olkaria marked by the eastern ring of domes (Naylor, 1972; Mungania, 1992; Clark et al., 1990). Gravity and seismic data do not show any indications of the presence of any caldera structure at Olkaria (Simiyu et al., 1998a; Ndombi, 1981). The occurrence of magmatic and gravity anomalies at the intersections of NE and NW rift faults is an

indication of distinct near surface heat sources controlling the reservoir characteristics of the geothermal system.

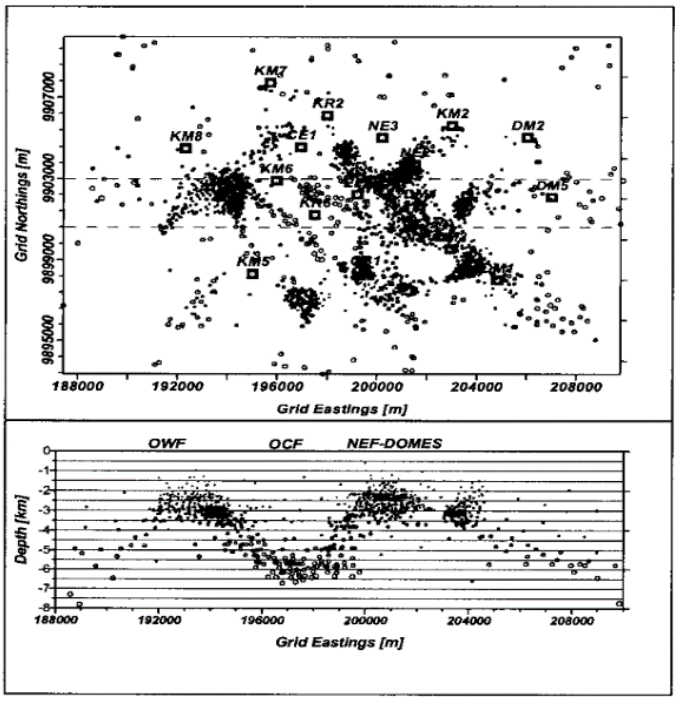

FIGURE 4: Location of microseismic events in the Olkaria field, recorded during a monitoring campaign in 1996-1998 (Simiyu, 2000)

Micro-earthquake monitoring for epicentre and hypocentre locations, Figure 4, shows that Olkaria is a high temperature geothermal field characterised by a high level of micro earthquake activity. The Olkaria West area has shallow high frequency events and deep low frequency events. The shallow events occur at the intersection of the Olkaria and Suswa faults. The shallow events are associated with an up-flow zone at the Olkaria West field. Shallow high frequency tectonic events and deeper low volcanic tectonic events occur within the East production field and NE-Olkaria along a NW-SE linear trend. The tectonic events that occur near the surface are associated with fluid movements and these volcanic tectonic events occur at the intersection of the Ololbutot fault zone and the Olkaria fault. Medium to deeper events occurring along the Ololbutot fault are linked to fluid movement at depth. Analysed temperature and pressure measurements, as well as the resistivity and the geochemical analysis, have shown that the fault is a recharge zone.

The S-wave attenuating bodies from the Micro seismic data collected during monitoring in the period 1996-1998 is an indication of the presence of partially molten material at depth. They coincide clearly with high productivity and the temperature regions of the Olkaria field as shown in Figure 5 (Mannvit/ÍSOR/ Vatnaskil/Verkís, 2011).

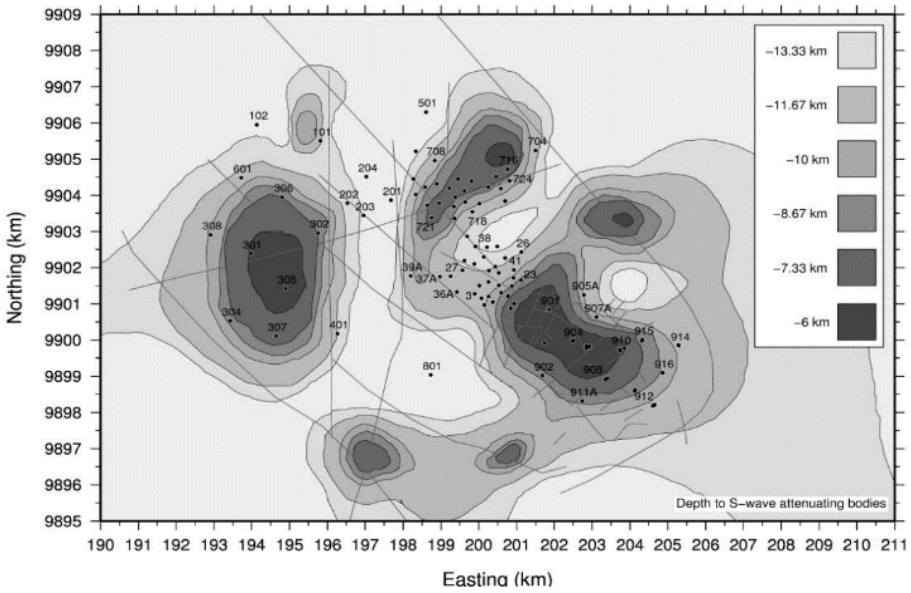

FIGURE 5: Depth to top of S-wave attenuating bodies in Olkaria geothermal field (adapted from Simiyu, 1998) (Mannvit/ÍSOR/Vatnaskil/Verkís, 2011)

A resistivity anomaly is clearly seen in the East, Northeast and West sectors in Olkaria (Figure 6). Low-resistivity anomalies are associated with up-flow zones where geothermal fluids flow along high permeability fracture zones. Resistivity structures show distinct northeast and northwest linear trends that are most likely due to alteration caused by geothermal fluid circulation along aligned fluid-filled fractures (Onacha et al., 2009).

The resistivity anomaly distribution at shallow depths is known to be in line with surface geothermal alteration. It is clear that a resistivity anomaly with NW-SE and NE-SW directions is structurally controlled. This explains that the structures that control geothermal fluid circulation are in the NW-SE and NE-SW directions. The shallow low resistivity anomaly is due to low temperature alteration followed by a resistive layer due to high temperature minerals and then a lower resistivity is interpreted as the heat source. Low resistivity anomalies, at depths of 1000 m a.s.l., define the geothermal resource. Some of the high resistivity coincides with the recharge areas associated with the NE-SW and NW-SE trending faults which act as conduits for cold water flow from the rift valley scarps. The geothermal fluid up-flow zones occur at the intersections of these regional faults and areas near the heat source. The resistivity anomaly in the Domes area does not manifest itself clearly with a weaker manifestation southwest of Olkaria (Maarita, 2009).

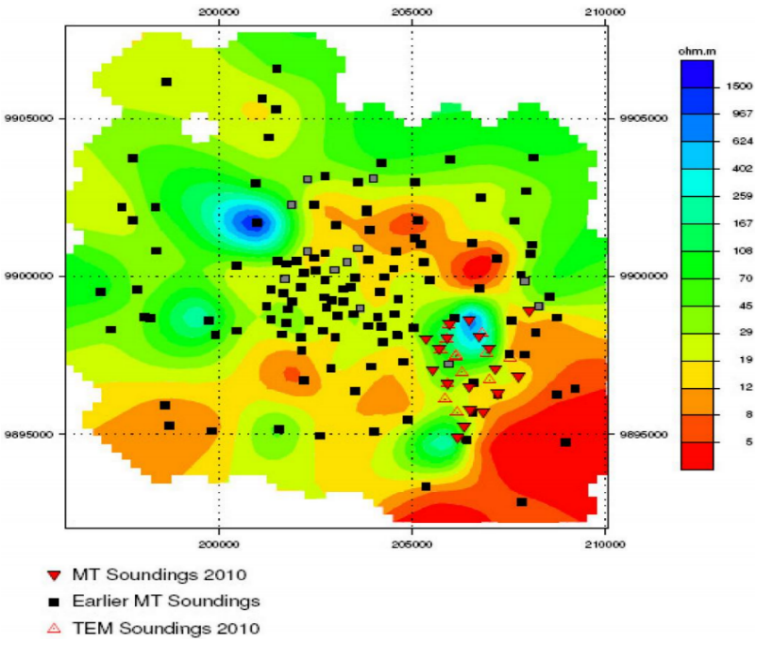

FIGURE 6: Resistivity map of Olkaria Domes field at -400 m a.s.l. (Wanjohi, 2011)

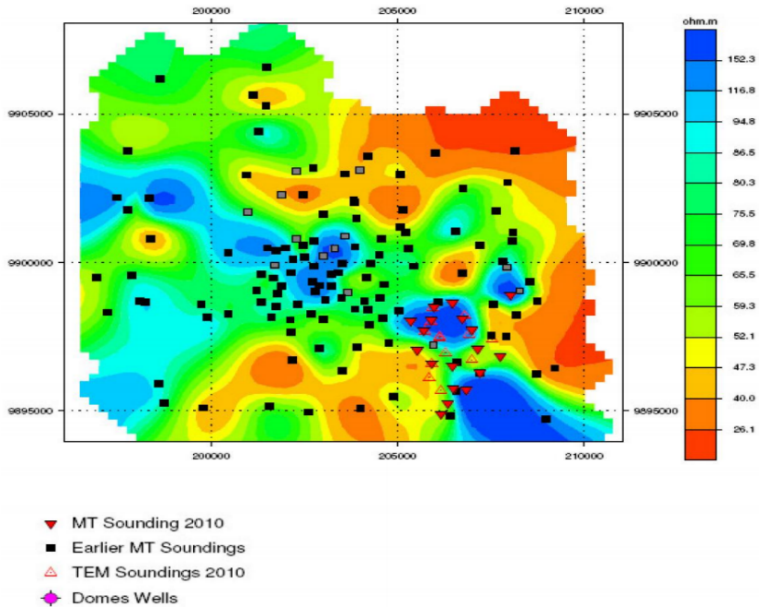

FIGURE 7: Resistivity map of Olkaria Domes field at 1600m a.s.l. (Wanjohi, 2011)

New resistivity data both for MT and TEM for Olkaria Domes field was analysed by Wanjohi in 2011 and the resistivity model is shown in Figures 6 and 7. This model indicates the extension of the geothermal resource in the southeast part of Olkaria because of the high resistivity mapped below the low resistivity (Wanjohi 2011), a common observation in high-temperature resources due to the high-temperature alteration.

2.3 Conceptual model development

The first conceptual model of the Olkaria geothermal field was developed by Sweco and Virkir (1976), based on data available at the time. The model was very simple because few wells had been drilled at the time. Sweco and Virkir postulated a boiling geothermal reservoir covered by a steam zone and restrained on the top by tuffaceous cap rock.

The recharge was believed to be meteoric water percolating down to 1600 m b.s.l. where it was heated to about 320°C. The hot water was then assumed to rise and eventually boil, with steam condensing below the cap rock; then the fluid fell to lower layers due to density differences where it was reheated in a convective cycle as shown in Figure 8.

Ofwona amended the model in 2002 by proposing two up-flow zones, one in the Olkaria Northeast field and another in the Olkaria East field, while the recharge was from all sides of Olkaria. Ofwona indicated that the Olkaria West field was not connected to the Olkaria East field but was separated by a low-temperature zone in central Olkaria. Extensive boiling also occurred in the up-flow zones to form steam caps below the cap rock. Figure 9 below shows the amended conceptual model by Ofwona.

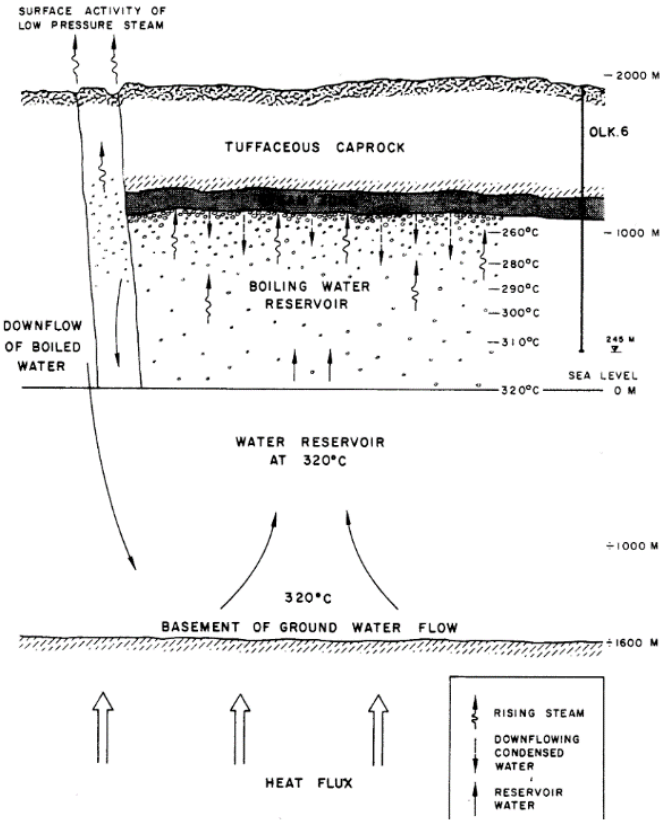

FIGURE 8: A simple conception model of the Olkaria Geothermal field (SWECO and Virkir, 1976)

West-JEC (West Japan Engineering Consultants, Inc.) further revised the conceptual model in 2009 (Figure 10) while undertaking a field optimisation study. They considered the origin of the heat source in the Olkaria geothermal system to be a magma chamber responsible for the volcanic activity in Olkaria. The magma chamber peaks in several locations, creating convective heat transfer and providing hot recharge to different parts of the geothermal system. They proposed an up-flow for the Domes sector through the R1 fault. The chemical model of all fields east of Ololbutot fault suggested that the fluids of all three sectors, East, Northeast and Domes field, had a common origin at depth, water between approximately 325-340°C in temperature with a chlorine concentration at ~450 mg/l. They explained that a common SE-NW trending structure, R1, may connect all three up-flow zones at great depths and may be extending northwards.

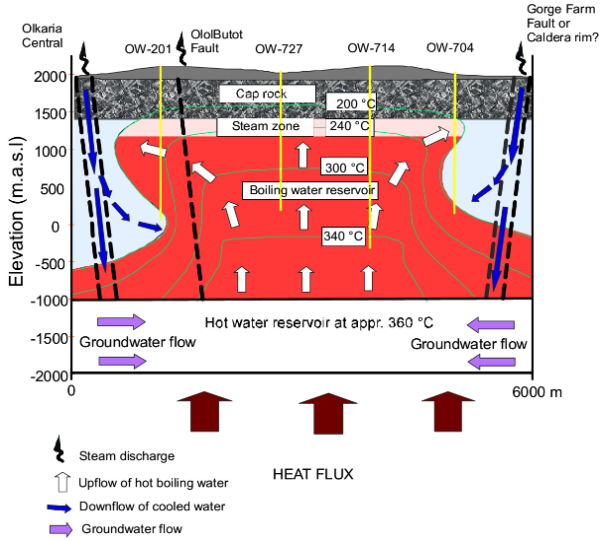

FIGURE 9: Olkaria conceptual model as presented by Ofwona (2002)

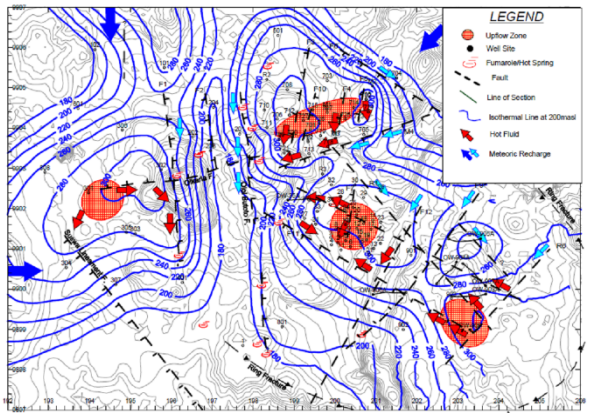

FIGURE 10: Olkaria conceptual model as presented by West-JEC (2009a)

The present conceptual model of the Olkaria geothermal system (Figure 11) was presented in 2012 by a consortium of Mannvit/ÍSOR/Vatnaskil/Verkís who undertook a field optimisation study as explained by Axelsson et al. (2013).

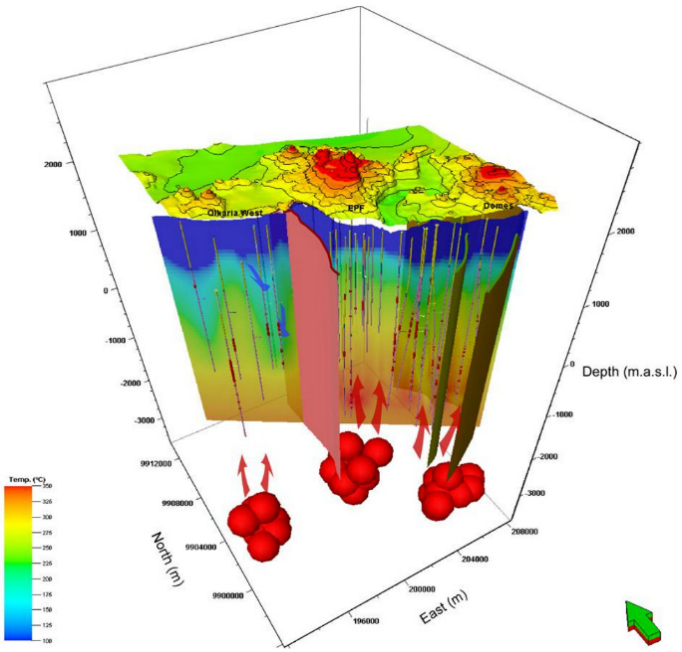

FIGURE 11: The present Olkaria conceptual model (Mannvit/ÍSOR/Vatnaskil/Verkís, 2011)

According to this model, the heat source is believed to be deep seated magma chamber or chambers with three intrusions 6-8 km from the surface, lying beneath the Olkaria hill, the Gorge farm volcanic centre and in the Olkaria Domes area. Four major up-flow zones were identified. The first feeds the Olkaria West field, believed to be connected with the heat source beneath Olkaria Hill.

Two major up-flow zones were identified as being connected to the Gorge farm heat source, one feeding the Northeast production field and another feeding the East field and the northeast corner of the Domes field. The fourth up-flow zone is associated with the ring structure in the Domes field, connected to the heat source identified below that area.

Permeability is believed to be controlled by NW-SE, NE-SW tending faults as well as the ring structure. Cold water flows into the system through the N-S tending Ololbutot fault which is a flow barrier between the western and eastern parts of the field. Water inflow into the Olkaria Domes area is believed to originate from the northeast part of the Domes field. They then concluded that the geothermal resource extended southeast of the field, based on the geochemistry, pressure and temperature data, and the geophysical data. They pointed out a possible resource in the south central and south west parts of Olkaria, indicated by limited geophysical data and surface manifestations.

From the discussions above, it is evident that the Olkaria field conceptual model underwent a transformation from a simple model presented by Sweco and Virkir (1976) to the more complex current model because of the continued collection of data, which gave a deeper understanding of the geothermal system. It is worth noting that the transformation underwent improvement, with the initial concept holding throughout the transformation process.

3. REVISION OF THE OLKARIA CONCEPTUAL MODEL

Optimal utilisation and expansion of geothermal resources is mainly dictated by reliable conceptual models which are updated with continued development and utilisation. They are the basis of field development plans and geothermal reservoir modelling (Axelsson et al., 2013). Conceptual models are descriptive or qualitative models, incorporating and unifying all available exploration, drilling and testing data (Grant et al., 1982).

Therefore, conceptual models are developed based on geological, geophysical, reservoir temperature and pressure as well as geochemical data. Monitoring data collected over time, during utilisation of geothermal resources, are used in updating conceptual models. The conceptual model explains the nature of the heat source, and the recharge zones; it describes the main flow channels as well as the general flow patterns in the reservoir.

3.1 New temperature and pressure data

Physical measurements made in geothermal wells provide the primary information from which the physical properties of a geothermal resource can be evaluated. The most important measurements are the temperature, pressure and the mass flow, made either in the well-bore or at the surface. During the first stages of resource development, an understanding of the resource in terms of its undisturbed state, size, rock characteristics, and pressure as well as temperature distribution is essential (Grant and Bixley, 2011).

New data has been acquired from the ongoing step out drilling operations and well testing in the Greater Olkaria Geothermal field. This includes both temperature and pressure measurement data as well as injection well test data. The discharge test data for a few wells are also available while most of the wells are still warming up after drilling. The temperature and pressure data for 28 wells has been analysed for this report. The drilling well data, such as the casing depth, casing shoe and conversion of the temperature and pressure measured depth to the true vertical depths, is also essential in understanding well design. The temperature and pressure profiles in this report are presented at the measured depth, while the elevations for the formation temperature and pressure are done in true vertical depth to allow comparison with the results of other reports on the field.

The temperature and pressure data were acquired through different well test operations using the Kuster temperature and pressure mechanical gauges. The temperature gauge uses a bimetal where the temperature expansion of the bimetal indicates the temperature. In this type of tool, the temperature measurements are not real time but recorded in a temperature probe on a clock driven recorder. An accuracy of more than ±1°C of the value is not achievable with the sensor, but they are superior to other sensors in that they can operate at higher temperatures, or up to 360°C. Pressure mechanical gauges, on the other hand, use the Bourdon tube where the fluids are in contact, hence sensing the pressure of the geothermal fluid at the measuring points. Their accuracy is between ±1 and ±0.1 bar of the measured value. These mechanical tools are regularly calibrated using a calibrating oil bath to ensure the accuracy of the measured data. A wire line assembly is used to lower the tools to the measuring depths.

The data used was obtained from various well test operations including well completion tests and temperature and pressure measured periodically during the warm up period. The well completion test involves first a temperature and pressure run immediately after stopping the water circulation in the drilling operation; it helps in understanding the temperature and pressure state of the well. This is followed by an injection test with pressure build-up and a pressure fall-off test to monitor the pressure response of the system due to changes in injection. This operation is commonly known as pressure transient analysis. The temperature and pressure profile, during pumping, maps out the zones of water loss during injection which corresponds to the points where the well is connected to the reservoir and may later indicate feed zones during production. The well's permeability can then be evaluated indirectly as well as the well's storativity.

3.2 Methodology

It is not possible to directly measure the subsurface well characteristics that are needed to assess a geothermal resource, as is the case in groundwater and the petroleum industry. An interpretation or an inference is made from the information available from a well test programme. The temperature and pressure were analysed, based on different models. The temperature models can be conductive, convective, isothermal, boiling conditions and one dimensional convection flows.

After well completion, geothermal wells are given time to recover from the cooling effect of the drilling fluids and to reach equilibrium with the formation. The temperature recovery behaviour is monitored during the warm up period so as to obtain information on the location of feed zones; the time series obtained are later analysed to estimate the natural undisturbed temperature of the system. The rate of

temperature recovery is dependent on the properties of the particular well as to whether the aquifers are warming up faster than the impermeable part of the well or vice versa. Usually, in static wells without internal flows or boiling conditions, the aquifers warm up more slowly than other parts of the well because of the cooling effects of the circulating drilling fluid.

Cross flow scenarios occur commonly in closed wells between the upper aquifers and the lower ones where flow comes into the well from upper aquifers and out through the lower aquifers. This type of well is characterised by a fairly constant temperature profile over a large depth interval in the well.

High-temperature wells sometimes experience boiling, where the fluid follows the boiling point with depth curve at some points in the well. Steam bubbles are formed and pushed upwards, warming the upper zones of the well where they are condensed and fall back by gravity, exhibiting one- dimensional convection behaviour.

Negative temperature gradient behaviour is also observed in geothermal wells. This is a situation where the temperature decreases with depth as a result of non-vertical water flow in the wells. This information can be used to locate horizontal flow patterns in geothermal fields (Stefánsson and Steingrímsson, 1990).

Formation temperature is an important parameter when understanding the nature of geothermal reservoirs during exploration, drilling, logging, well completion and reservoir analysis. The subsurface temperature available from borehole well logs is always lower than the true or static formation temperature, because of the cooling effect of drilling fluids. In Olkaria, it is not always possible to allow sufficient time for the wells to heat up before discharge because of operational constraints. Furthermore, penetration of a steam zone during drilling results in the masking of temperatures at shallower depths, hence making it difficult to estimate the true formation temperature in this region.

Various techniques have been developed to obtain true formation temperatures from transient data (Dowdle and Cobb, 1975; Barelli and Palama, 1981). James N. Albright developed a method (Albright method) for calculating the formation temperature during economical interruptions of drilling operations while a geothermal test well was being drilled for the *Hot Dry Rock geothermal energy project* conducted by the Los Alamos scientific laboratory. Further details of this method can be obtained from The User's Manual by Arason et al. (2004).

A simple and effective method was published by Roux et al. (1979), based on the Horner time. The basic concept is the straight line relationship on a semi logarithmic scale of measured temperature versus the ratio of the Horner time, τ:

$$\tau = \frac{\Delta t}{(t_c + \Delta t)} \tag{1}$$

where Δt is the time in hours after stopping circulation and t_c is the circulation time in hours.

The static formation temperature, T_{ws} is extrapolation from the straight line relationship to Horner time $\tau = 1$.

Berghiti (Arason et al., 2004.), a computer program based on the Horner time method, was used for this project during the formation temperature estimation. The following procedure was used on making a decision on the applicable part of the geothermal wells:

1. The temperature values of the well less than 50 m from the well bottom were not used because circulation might not have been effective in this region;
2. Only sections of conductive heat transfer were considered;
3. Sections with indications of flow between different sections, internal circulation and cross-flow in the wellbore were not used.

The condition of geothermal fluids at zones penetrated by some of the wells is liquid at greater depths and is at specific temperatures referred to as the saturation temperature. As the fluid flows up the wells, the pressure reduces until a saturation temperature is reached where boiling occurs. This means that the formation temperature can be assumed to follow the saturation curve at depths where the fluid is believed to be at the saturation temperature. The pressure in geothermal wells is equivalent to the hydrostatic gradient plus the dynamic gradient at some point in the well where the liquid is at saturation temperature. The dynamic gradient is much smaller than the hydraulic gradient and the pressure can be approximated by Equation 2 below:

$$\frac{dp}{\mathrm{dz}} = \rho_{\mathrm{w}} \mathrm{g} \tag{2}$$

Equation 2 can be used to calculate the boiling point depth curve for the saturation conditions by numerically solving Equation 3 (Arason et al., 2004):

$$P(z) = \mathrm{P_o} + g \int_{z_o}^{z} \rho_{\mathrm{sat}} dz \tag{3}$$

The formation pressure can therefore be determined from the formation temperature for the part of the well which is at boiling conditions by calculating the saturation pressures at that temperature. The boiling point depth curve was formulated in this report by considering the water level and using BOILCURVE, a computer program in Icebox (Arason et al., 2004) for calculating the boiling point curve. PREDYP, another program in Icebox (Arason et al., 2004), which calculates the pressure in a static water column as a function of measured temperature and water density, was also used to estimate the formation pressure.

3.3 Updated temperature and pressure models

The temperature and pressure models discussed in the previous chapter were formulated based on all the available temperature and pressure measurements for a given well. The effects of boiling and internal flows are taken into account while estimating the initial temperature and pressure at the point of the system in the well. The new wells drilled in the Greater Olkaria geothermal field used in the project are shown in blue in Figure 12. Also shown are the older wells which were analysed earlier. The temperature and pressure profiles of the new wells incorporated with their estimated formation temperatures are shown in Appendix I, with a few examples discussed below.

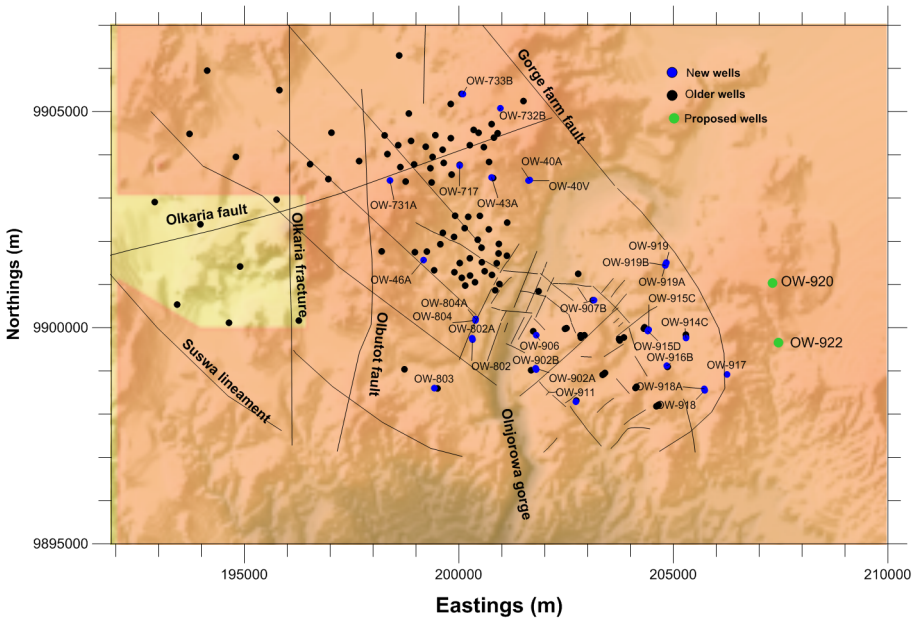

FIGURE 12: Geothermal wells in the Greater Olkaria geothermal field

Figures 13, 14 and 15 give the temperature and pressure estimates in Wells OW-918A, OW-917 and OW-918, respectively, located in the southeast part of Olkaria Domes field as shown in Figure 12.

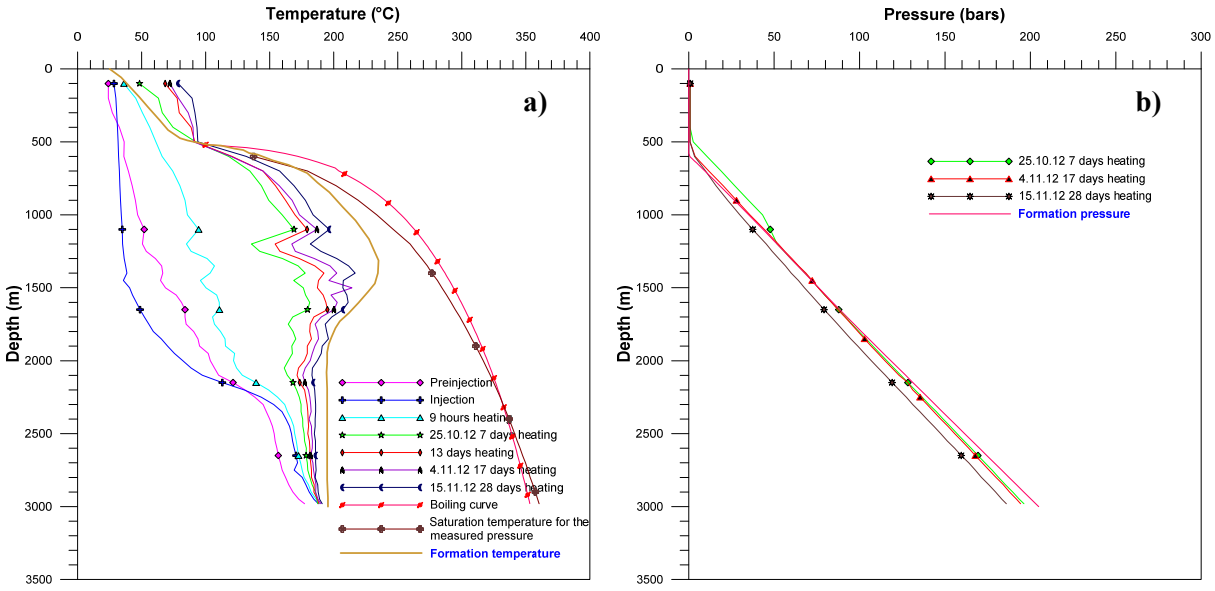

FIGURE 13: Well OW-918A: a) Temperature profile; and b) Pressure profile

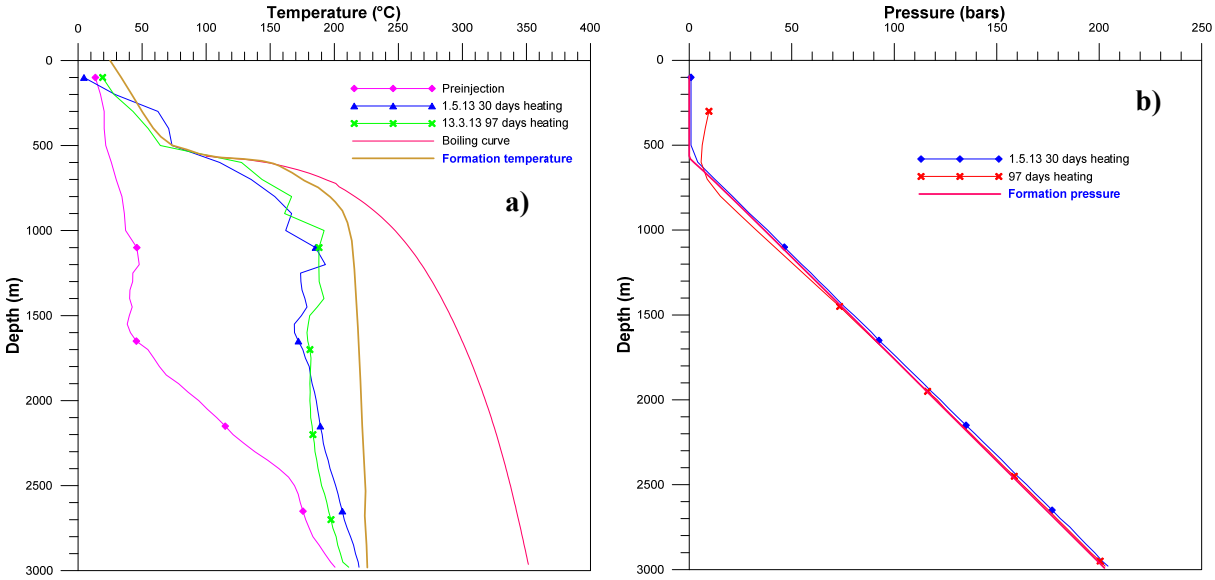

FIGURE 14: Well OW-917: a) Temperature profile; and b) Pressure profile

The temperature profile in Well OW-918A shows a high gradient up to a depth of 1300 m from the surface, then a temperature reversal to the well bottom. The formation temperature estimates to about 250°C at 1300 m and then reduces to 210°C at the well's bottom.

Conductive heating is evident in Well OW-917 to the well bottom, which is an indication of poor permeability. Well OW-918 also shows conductive temperature recovery to about 1300 m, then isothermal conditions to 2150 m, followed by a slight temperature reversal before another level of conductive heating to the well bottom.

The pressure profiles in Wells OW-918A and OW-917 show a water table at around 600 m, while in Well OW-918 a water table at around 500 m was observed. In Wells OW-918A and OW-917, estimated formation pressure shows a water table at around 600 m, while in Well OW-918, a water table at around 500 m was observed.

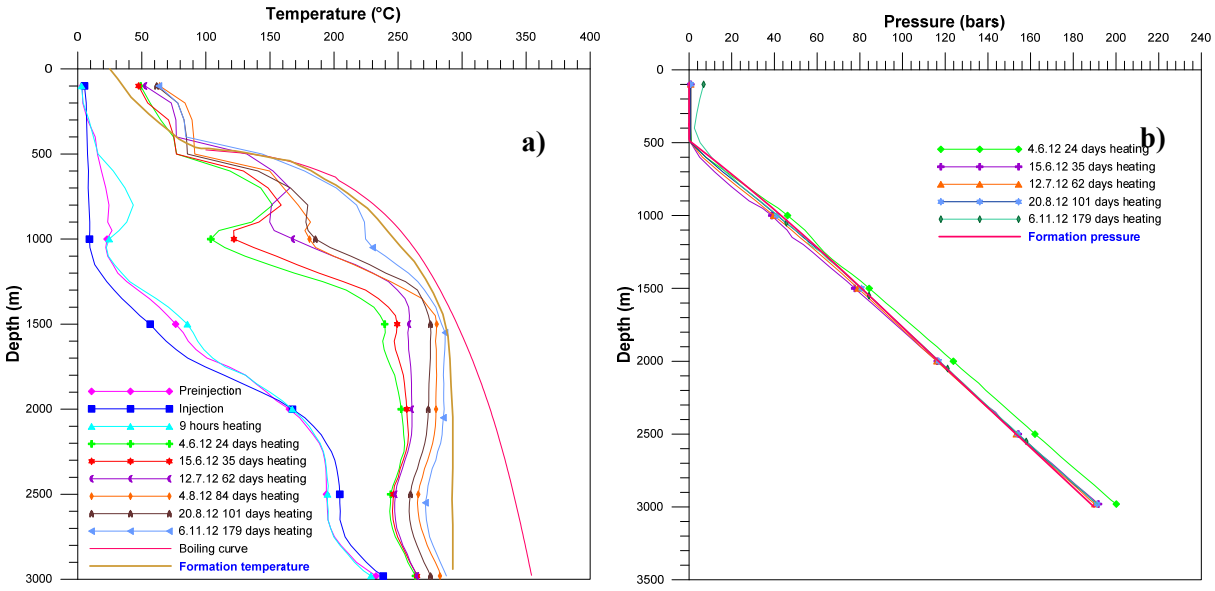

FIGURE 15: Well OW-918: a) Temperature profile; and b) Pressure profile

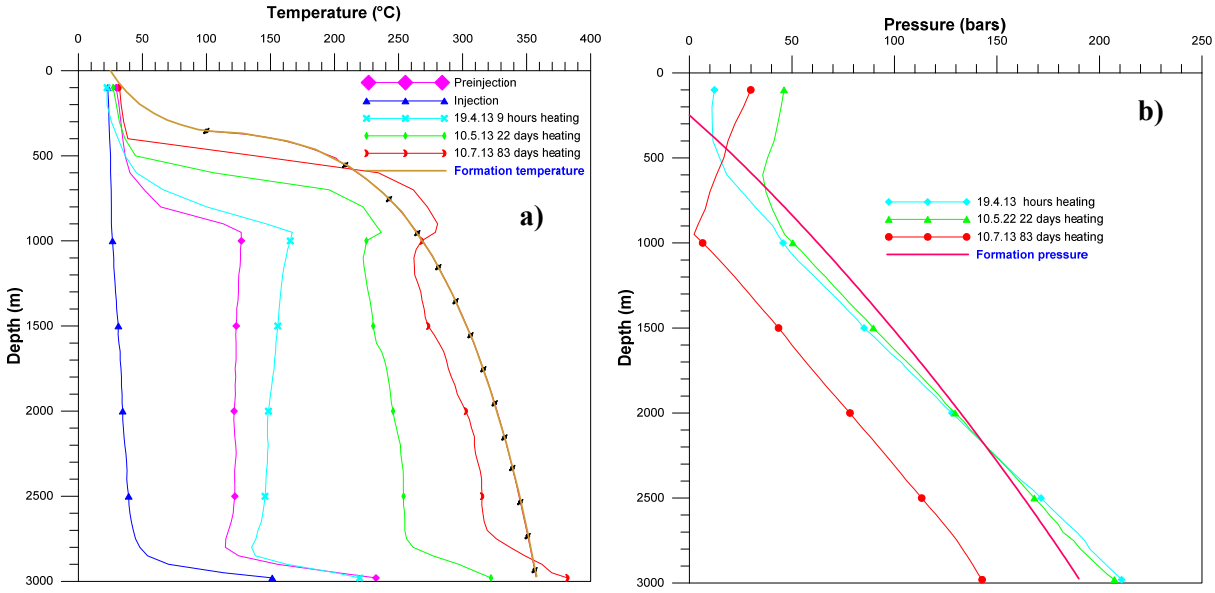

FIGURE 16: Well OW-919A: a) Temperature profile; and b) Pressure profile

Well OW-919A is a very hot well drilled in the eastern part of the Olkaria Domes field with temperatures of about 350°C at the well bottom and a pressure close to 200 bars (Figure 16). The formation temperature in the well follows the boiling point curve to the well bottom.

Figure 17 and Figures 1 and 2 in the Appendix I show the temperature profiles in Wells OW-731A, OW-717, and OW-732B, respectively, located in the NE production field as shown in Figure 12. The temperature is observed to increase to a peak of 230°C at around 1100 m, then reverses sharply to 190°C, followed by normal temperature gradient to the well bottom in Well OW-731A.

A temperature reversal is also seen in Well OW-732A where the estimated formation temperature increases to about 300°C at around 2000 m from the surface, then suffers a reduction to 250°C at the well bottom with a low discharge enthalpy of 1060 kJ/kg. Well OW-717 also records lower temperatures

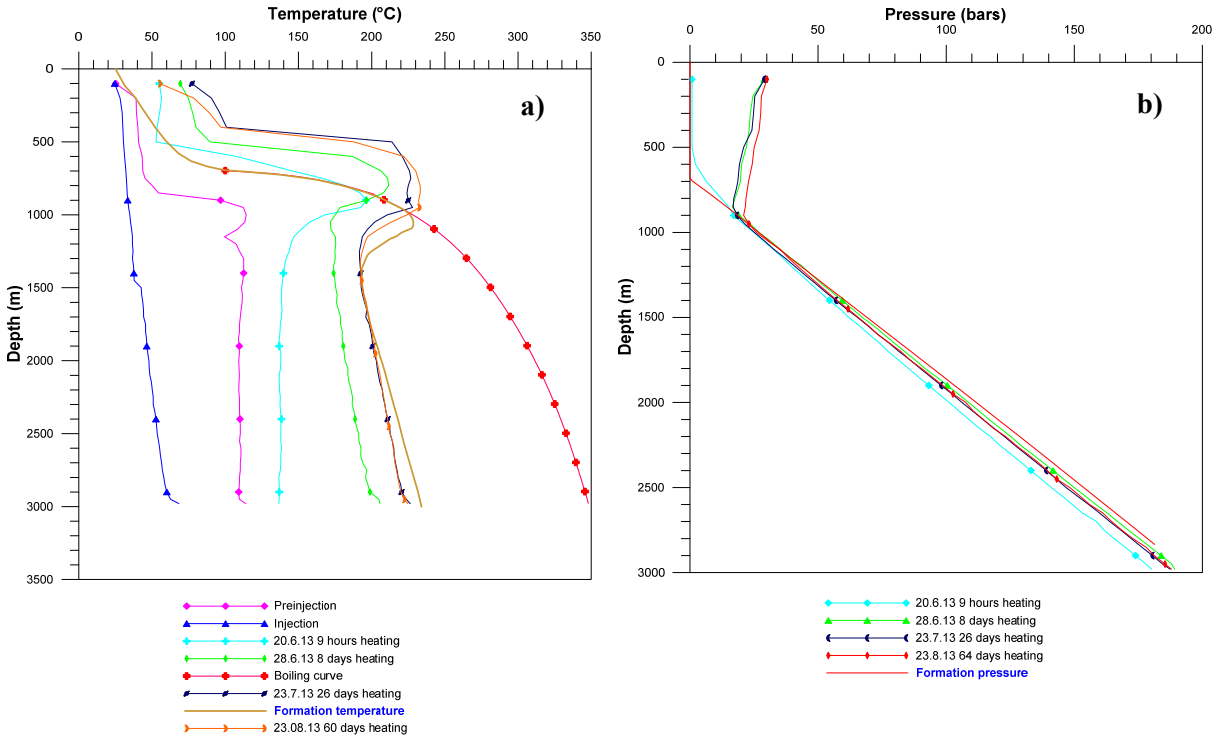

FIGURE 17: Well OW-731A: a) Temperature profile; and b) Pressure profile

than nearby, but shallower, wells with a low enthalpy of 1580 kJ/kg, similar to old Well OW-717 which was drilled in the same region.

Well OW-733B (Figure 18) in the northern part of the Olkaria Northeast field shows high temperatures of close to 370°C at the well bottom with the estimated formation temperature following the boiling

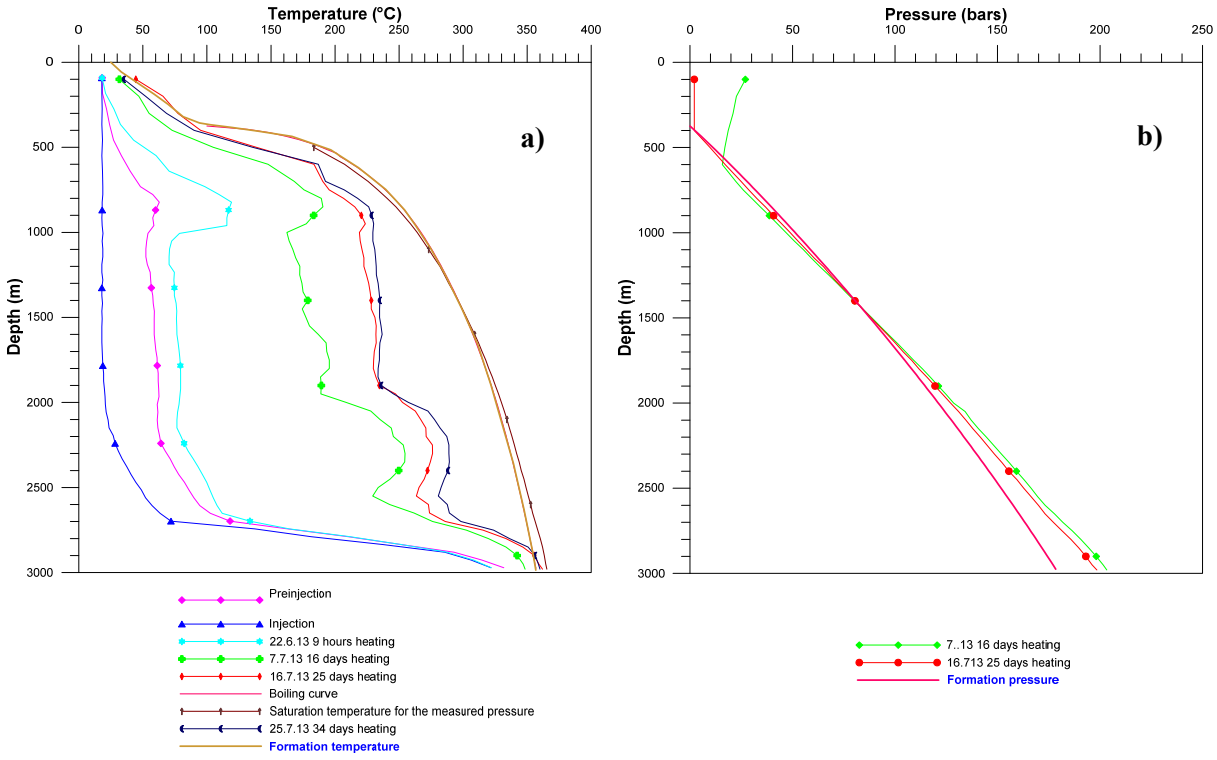

FIGURE 18: Well OW-733B: a) Temperature profile; and b) Pressure profile

point by depth curve. Wells OW-43A and OW-46A (Figures 3 and 4, respectively, in Appendix I) in the Olkaria East field show boiling conditions at 800 m depth and high discharge enthalpy of 2428 and 2085 kJ/kg recorded, respectively, thus the formation temperatures were interpreted to follow the boiling point with depth curve. Wells OW-40V and OW-40A were drilled in the eastern part of the East production field, bordering the Northeast production field, as shown in Figure 12 above. Low temperatures were recorded in these wells with alteration minerals showing inflow of cold water into Well OW-40V. However, slightly higher temperatures were observed in Well OW-40A which was drilled directionally to the east; the well has high pressures and good permeability to a few metres from the well bottom. Figures 5 and 6 in Appendix I show the temperature and pressure plots in Wells OW-40V and OW-40A, respectively.

The temperature and pressure profiles for the Southeast field are shown in Figures 7-11 in Appendix I. Generally, low pressures were recorded in the wells. Well OW-802 recorded temperatures of up to 290°C at the well bottom with the estimated formation temperature following the boiling point with depth curve to around 1450 m. Boiling was observed in Well OW-802A above 1000 m and the main feed zone shown by the injection temperature profile is located at around 1950 m. Conductive heating is generally observed in Well OW-803 while Well OW-804 also shows boiling above 1000 m.

The temperature and pressure models are presented as cross-sections across selected areas considered to be of interest and where additional data was acquired. Five planar sectional views were also made so as to understand the heat and pressure distributions at different elevations in the field. The formation temperature and initial pressure estimates done by the Mannvit/ÍSOR/ Vatnaskil/Verkís consortium in 2011 and 2012a were also included so as to have a clearer picture of the field.

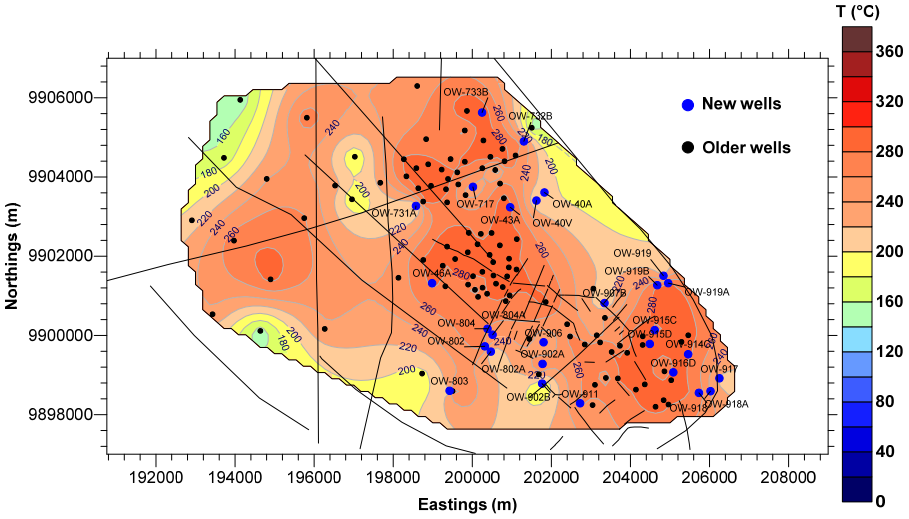

FIGURE 19: Temperature distribution at 800 m a.s.l. elevation

Figures 1 and 2 in Appendix II show temperature and pressure contour maps for the Olkaria geothermal field at 1200 m a.s.l., respectively, while Figures 19-26 show the temperature and pressure iso-maps across the Olkaria field at 800, 400, 0 and -400 m a.s.l., respectively. In

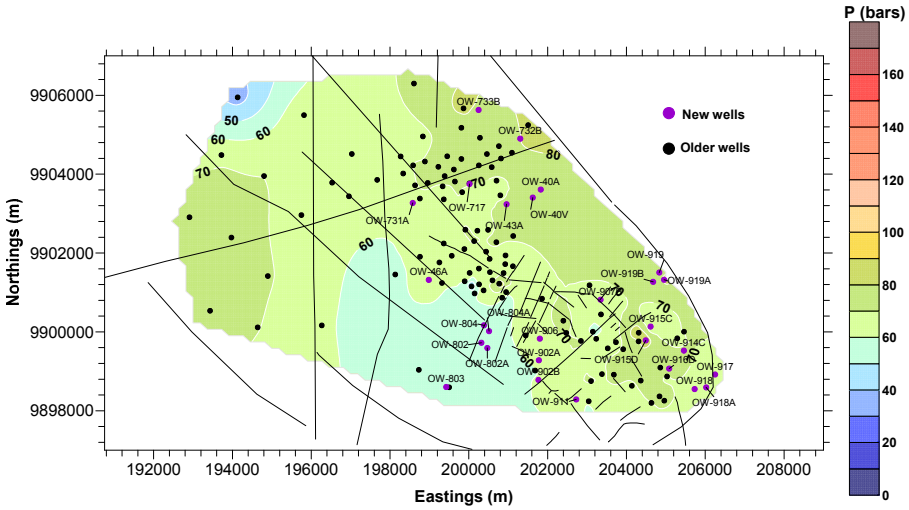

FIGURE 20: Pressure distribution at 800 m a.s.l. elevation

the figures below, the new wells are shown in blue and the older wells are shown in black.

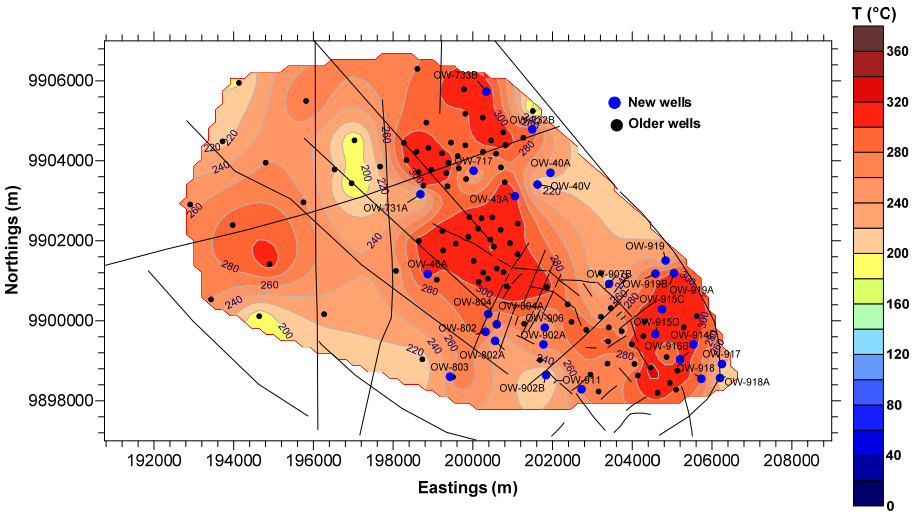

FIGURE 21: Temperature distribution at 400 m a.s.l. elevation

The temperature distribution in the field at an elevation of 800 m a.s.l. shows cooling around Well OW-731A which could be close to the boundary of the cold Ololbutot fault around Well OW-201 and the Northeast production field. Slight cooling is evident towards Well OW-717 which could mark the boundary of the Northeast and East production fields along the Olkaria fracture to Wells OW-40V and OW-40A. This trend is also observed at elevations of 400, 0, and -400 m a.s.l. The isotherms in the southern part show high temperature around this area, separated from the Domes field by a lower temperature around Well OW-902B.

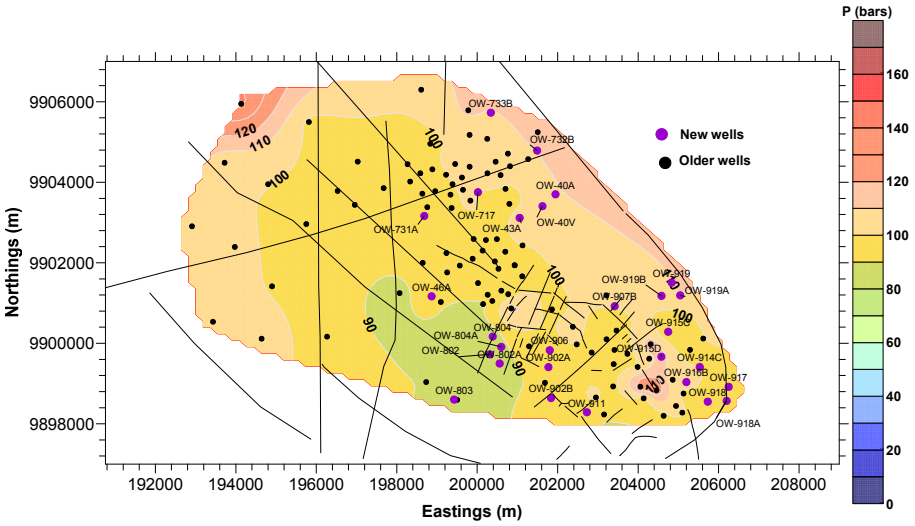

FIGURE 22: Pressure distribution at 400 m a.s.l. elevation

The southeast part of Domes shows cooling around Well OW-918A where the isotherms are observed to move gradually to a few depths from the surface from all other parts of the Domes field area towards the location of Wells OW-914 and OW-915 and extend eastward, indicating that the main up-flow zone for Olkaria Domes field is located in the region. Slight cooling was observed around Wells OW-910 and OW-909.

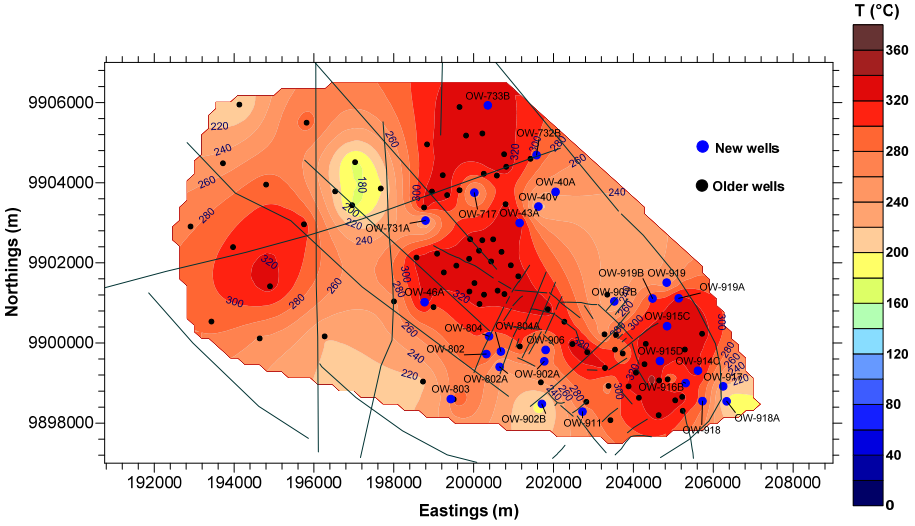

FIGURE 23: Temperature distribution at sea level

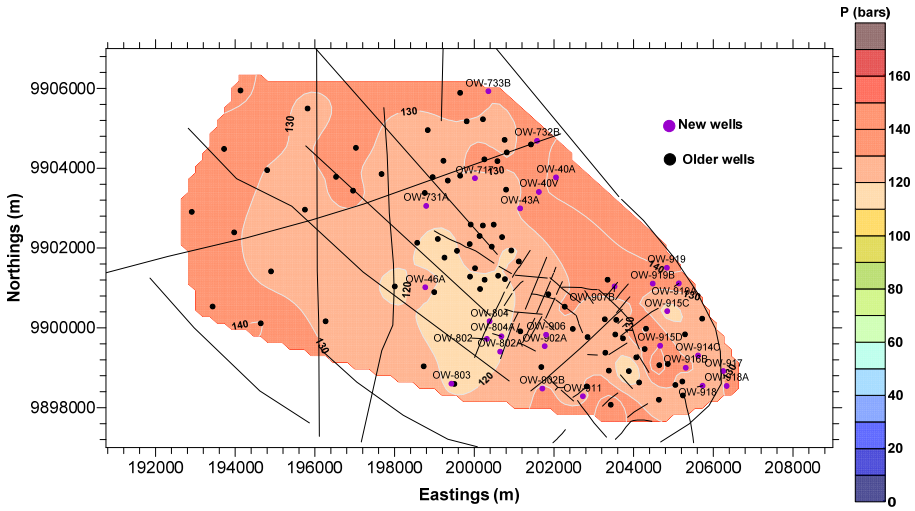

FIGURE 24: Pressure distribution at sea level

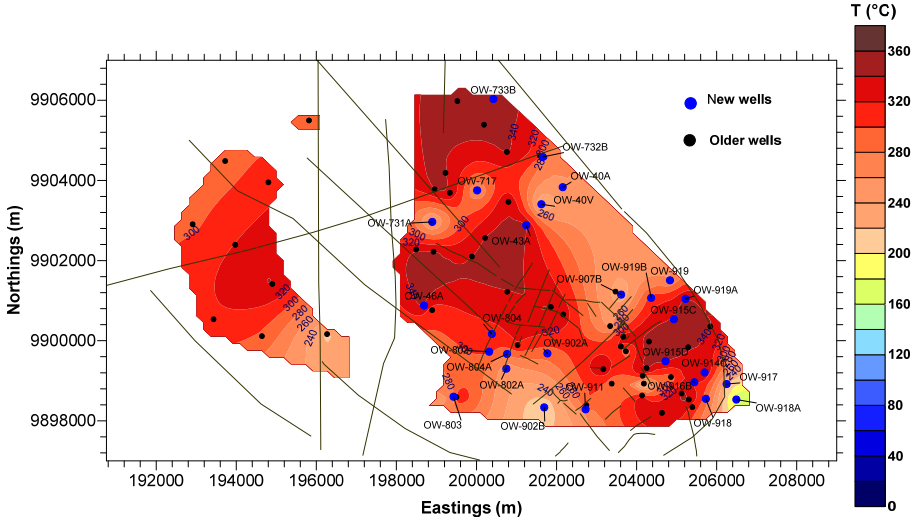

FIGURE 25: Temperature distribution at
-400 m a.s.l. elevation

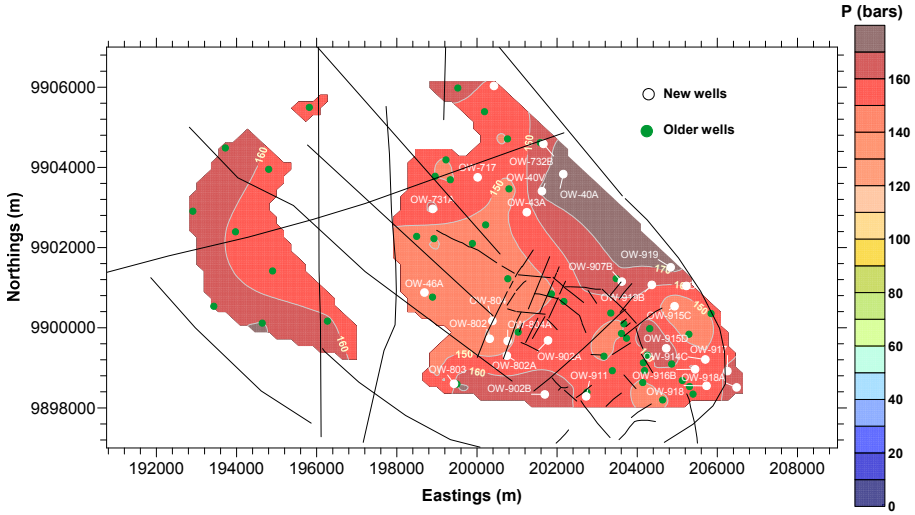

FIGURE 26: Pressure distribution at -400 m a.s.l. elevation

It is also evident, from the isotherms at 1200 m a.s.l. and 800 m a.s.l., that a higher temperature region is shallower in the East production field than in the Domes field. The isomaps show the pressure is lowest in the southern part of the Olkaria field.

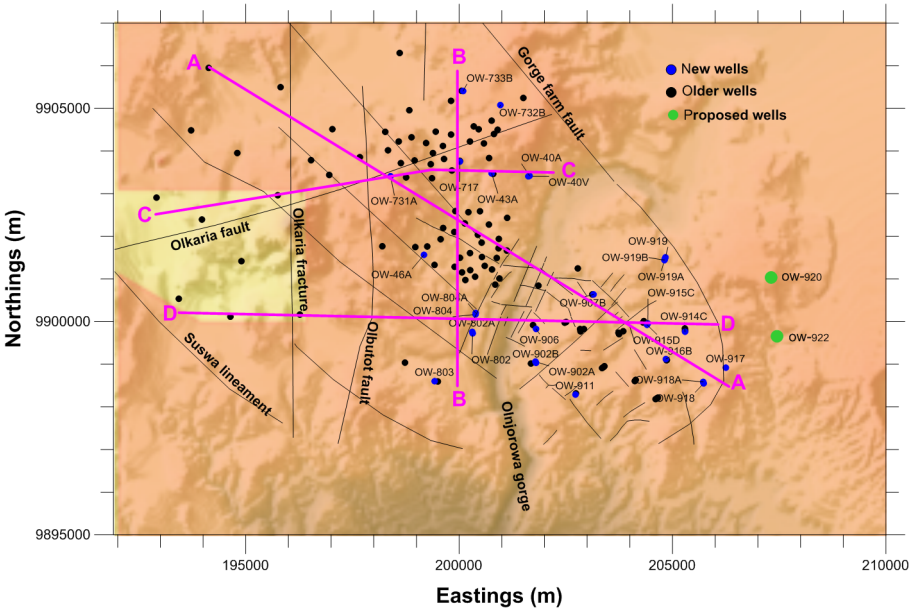

FIGURE 27: Map showing well locations and cross-sections across the Olkaria geothermal field

Four cross-sections were made for the analysis of the vertical temperature and pressure models of the Olkaria geothermal system. Figure 27 shows the location of the different cross-sections, AA, BB, CC, and DD.

Figure 28 shows the temperature and pressure in cross-section AA from Well OW-102 in the Olkaria South West field through to Wells OW-731A and OW-38 to OW-917 in the southeast part of Olkaria Domes field. The isotherms are depressed west of Olobutot fault with the 160°C isotherm reaching a depth of 0 m a.s.l., indicating cooling in that part of the field. A possible cooling was also observed around Well OW-731A.

The isotherms drastically rose to a shallower depth as the Northeast production field was crossed with the 200°C isotherm at around 1650 m a.s.l. The isotherm went slightly deeper as the East field was crossed to a depth of 1500 m a.s.l. around Wells OW-38 and OW-41, located at its main up-flow zones. The isotherms are then depressed to a depth of around -100 m a.s.l., crossing Well OW-907A in the Domes production field. Moving to the main up-flow zone in the Domes field, located around Wells OW-915 and OW-916, the temperature line approaches the surface at a depth of 1650 m a.s.l. Cooling is possibly occurring in around Well OW-918A in the southeast Domes, as indicated by the depressed 201°C isotherm at a depth of around -600 m a.s.l.

The pressure isolines for cross-section AA (Figure 28b) display the same pattern, peaking at the perceived up-flow zones and dipping at the regions experiencing cooling.

Cross-section BB runs from Well OW-803 in the south to Well OW-733B in the north, passing through Well OW-717. Figure 29 shows a slight movement of the isotherms near the surface as you cross from the south to the centre of the East production field. Slight cooling was observed around Well OW-717 but the isotherms move close to the surface in the north. A similar pattern was observed in the pressure contour lines (Figure 29b).

Figure 30 shows cross-section CC, starting at Well OW-308 in the west reaching to the northeast to Well OW-717, then to the east to Well OW-40A. Cooling was also observed to the west of the Ololbutot fault with slight cooling around Well OW-717 (Figure 30a). Another indication of cooling was seen in Well OW-40V but the hot contour moved to a shallower level as it approached the Gorge farm fault through Well OW-40A.

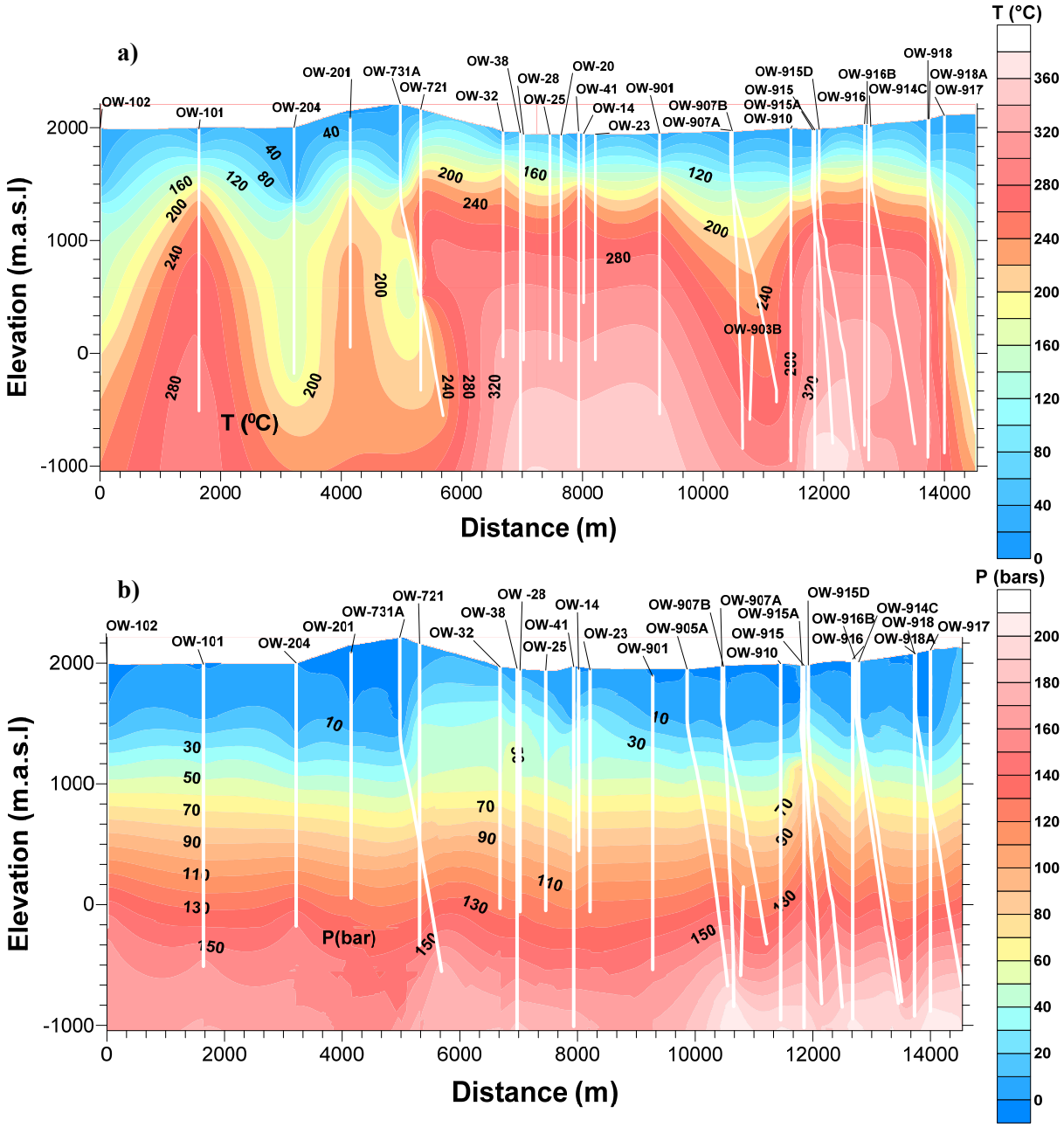

FIGURE 28: Cross-section AA: a) temperature profile; and b) pressure profile

Another cross-section of interest is section DD (Figure 31) from Well OW-304 in the West field to Well OW-914 in the Domes field. Figure 31a shows that cooling was observed to the west of the Ololbutot fault, as observed in the previous sections, but moved gradually closer to the surface from Well OW-802 to Well OW-914 in the East field. A similar pattern was observed with the isobars dipping near the Ololbutot fault (Figure 31b).

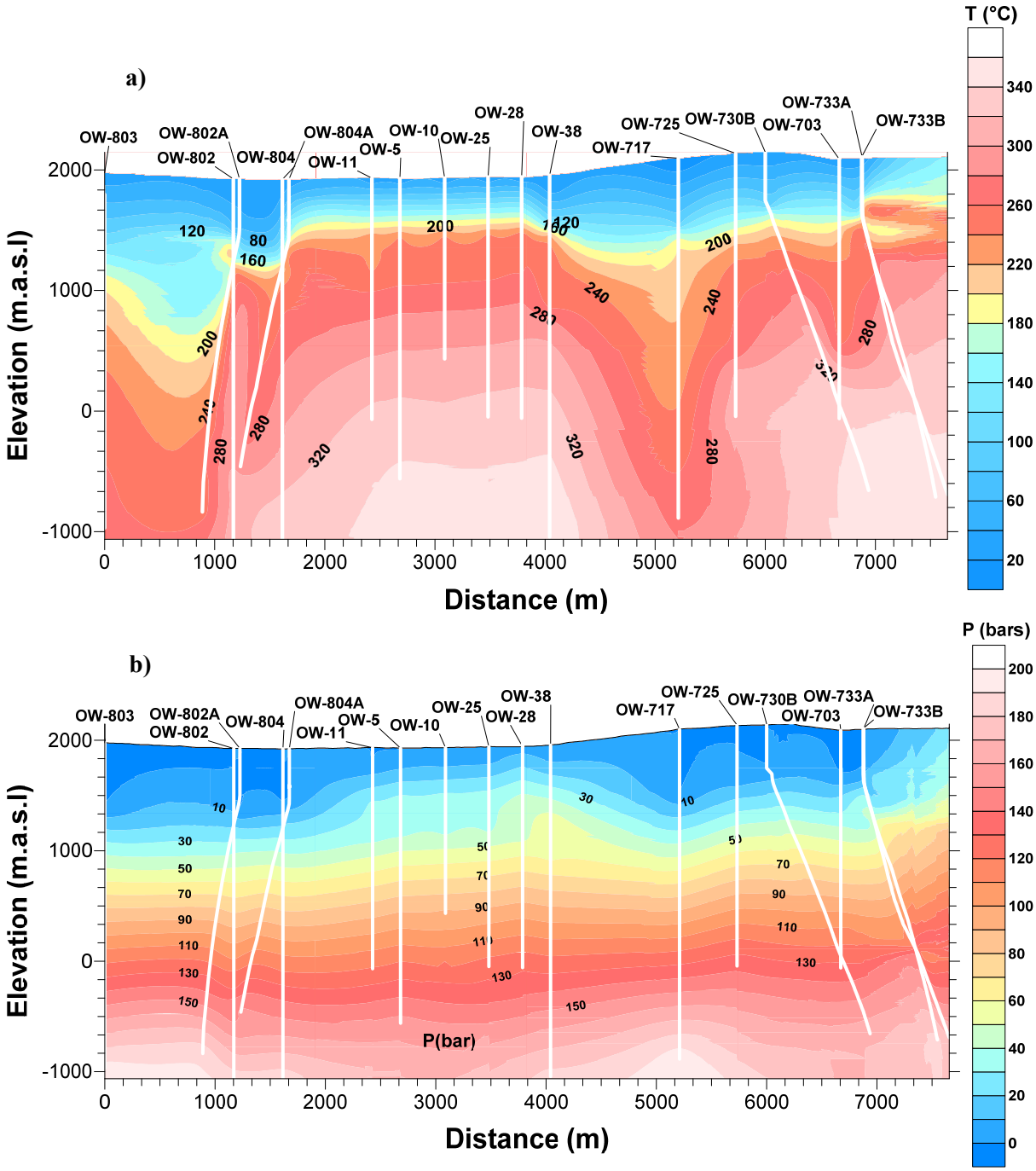

FIGURE 29: Cross-section BB: a) temperature profile; and b) pressure profile

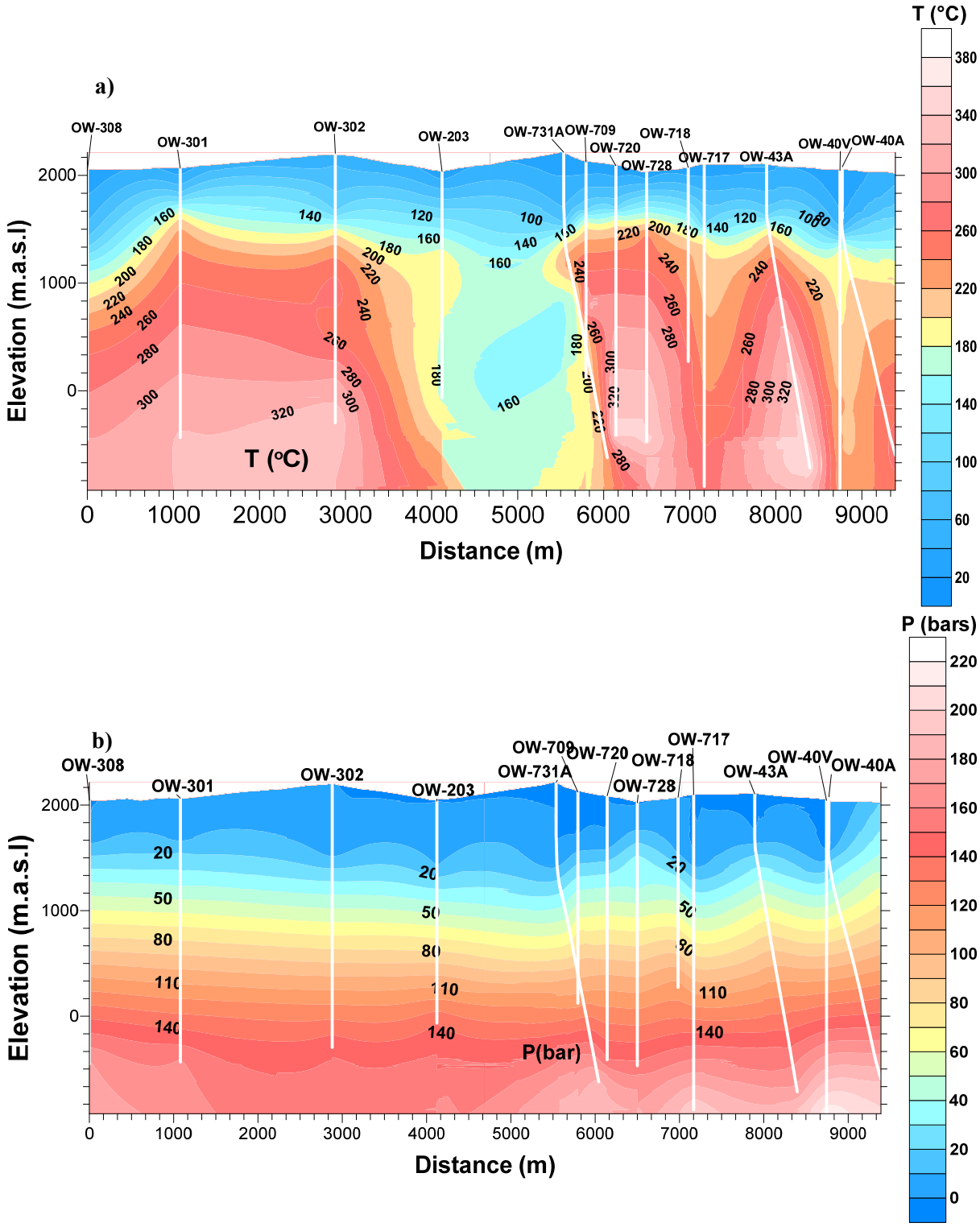

FIGURE 30: Cross-section CC: a) temperature profile; and b) pressure profile

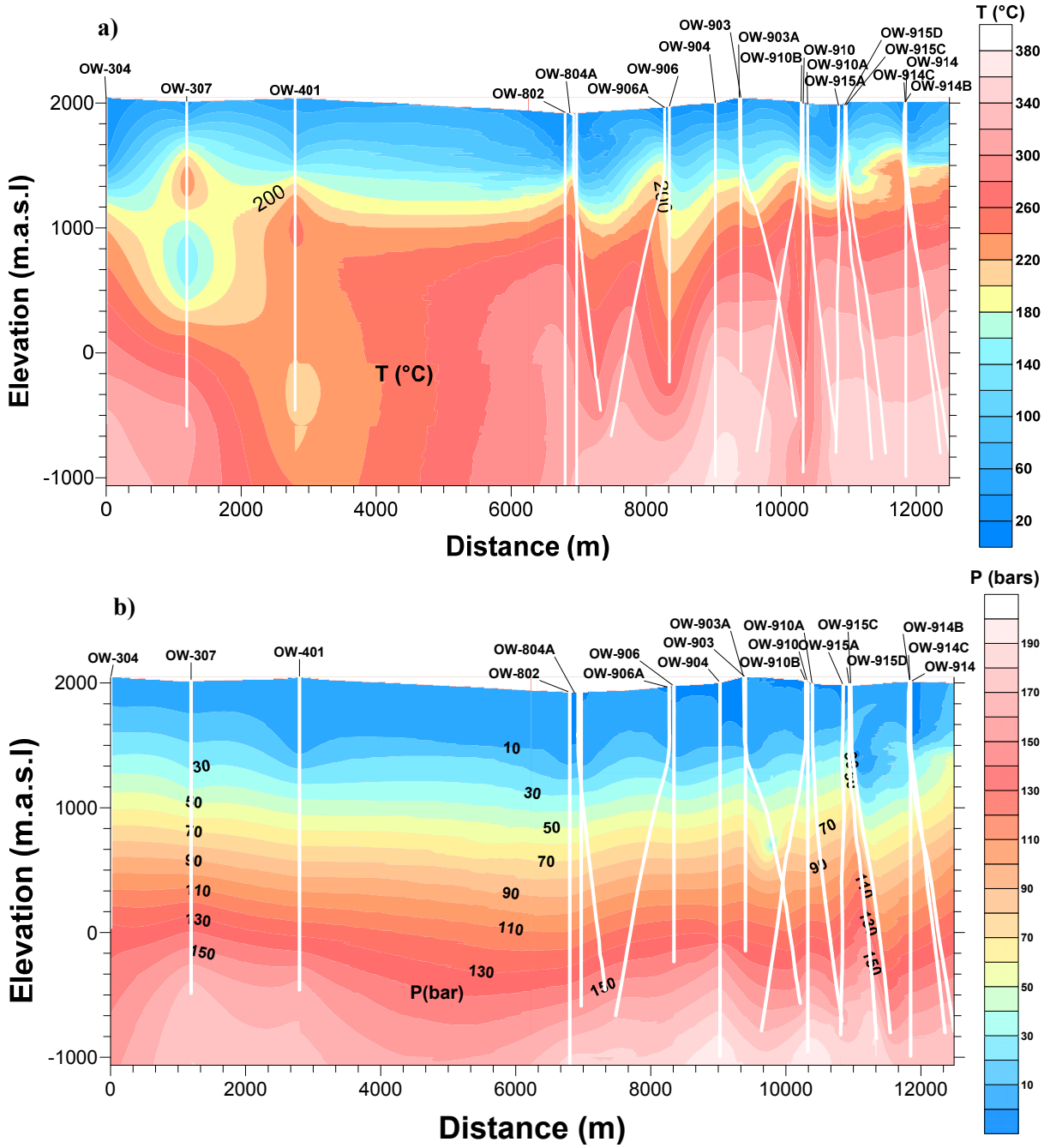

FIGURE 31: Cross-section DD: a) temperature profile; and b) pressure profile

3.4 Revision of the conceptual model

The development of reliable conceptual models requires a multi-disciplinary approach where the varying dimensional concepts of different geosciences involved in the exploration and development are put together. Conceptual model development requires the understanding of the nature and size of the heat source, the fluid recharge to the system and the up-flow zones, the main permeable regions of the system, the initial temperature and pressure conditions of the system and the nature of the boundary conditions.

The present work looks at the possible changes in the Olkaria geothermal field conceptual model as developed by the consortium of Mannvit/ÍSOR/ Vatnaskil/Verkís, based on the interpretation of newly

acquired temperature and pressure data and the accompanying updated temperature and pressure model. The geology and the geophysical information, as analysed and described by Mannvit/ÍSOR/ Vatnaskil/Verkís (2011), played a key role in interpreting the data as well as in developing the temperature and pressure models. New additions to the conception model are pointed out as follows:

1. The geothermal resource possibly extends north of the Olkaria Northeast production field, confirmed by very high temperatures of over 360°C in Well OW-733B, newly drilled in the area.
2. The immediate eastern part of the East production field is possibly a down-flow zone or low temperature region but, further east towards the Gorge farm fault, temperatures are increasing, indicating a possible up-flow zone.
3. The area near Wells OW-717 and OW-731A indicates a down flow zone that could indicate the boundary of the East field and the Northeast field, as well as cooling in the region.
4. The eastern part of Domes field is a high-temperature and pressure up-flow zone; the boundary was not demarcated by Wells OW-914B and OW-914C, recently drilled in the area. Both wells show high temperatures, as seen in Figure 31a.
5. The wells already drilled in the southeast part of the Olkaria Domes field indicate very poor permeability in a small area, as shown by the localised high-resistivity anomaly in Figure 6 in Section 2.2. Further east of the spot with a high resistivity anomaly, down-flow conditions are encountered. Well OW-918A, drilled across the ring structure southeast of Domes field across an area where the ring structure curves towards the west, indicates a temperature reversal at the well bottom, a result of a possible horizontal flow in the region. Further southeast, a low resistivity anomaly is encountered which could be the result of a possible up-flow zone.

Figure 32 shows a pictorial view of the revised conceptual model.

It is believed that three major heat sources are within the Olkaria geothermal system. These are magma intrusions from deep lying magma to a depth of 6-7 km from the surface. The heat sources are located below the Olkaria hill, the Gorge farm volcanic centre, and below Olkaria Domes field. The one below the Olkaria hill is responsible for the up-flow zone in the western part of the field and is shown in Figure 32, marked in red to the left.

The heat source located at the Gorge farm volcanic centre is associated with the up-flow zone for Olkaria East and Olkaria Northeast fields, as shown by the red arrow in Figure 32, indicating conduction from this heat source to the Olkaria East up-flow zone. The red body to the right in Figure 32 represents the heat source beneath Olkaria Domes field. Heat is then conducted to a deep reservoir located near the up-flow zones for each field, as shown by the orange arrows. Cold down flow is proposed to come from the Ololbutot fault and the ring structure in the southeast part of the Domes field down to this hot region, thus forming a hot water reservoir beneath each up-flow zone for the different fields.

Four major up-flow zones are connected to this deep reservoir through NW-SE and NE-SW trending faults. These four major up-flow zones are confirmed by the temperature and pressure contour maps in Section 3.3. The pressurised hot water flows upwards through faults and fractures and some move all the way to the surface as fumaroles and hot springs. The reduced pressure in Olkaria East and Olkaria Northeast fields, as the water rises to shallower levels, results in boiling, thus forming a steam cap near the cap rock.

In the wells drilled in the Domes field, which had a chance of intersecting these fractures, the pressurised water enters the wells and boils in the wells as they rise up when the wells are opened, yielding two phase steam and water on the surface.

Another up-flow zone is proposed beyond the down flow in the southeast part of the Domes field that may be associated with the heat source beneath the Olkaria Domes field. There could be fractures and faults that connect to a possible hot water reservoir associated with this heat source, thus forming a reservoir in this part of the field. This is shown by the low resistivity of 12-29 Ωm in the vicinity of a conductive zone of 0-12 Ωm, associated with good productive areas in the Olkaria Domes field.

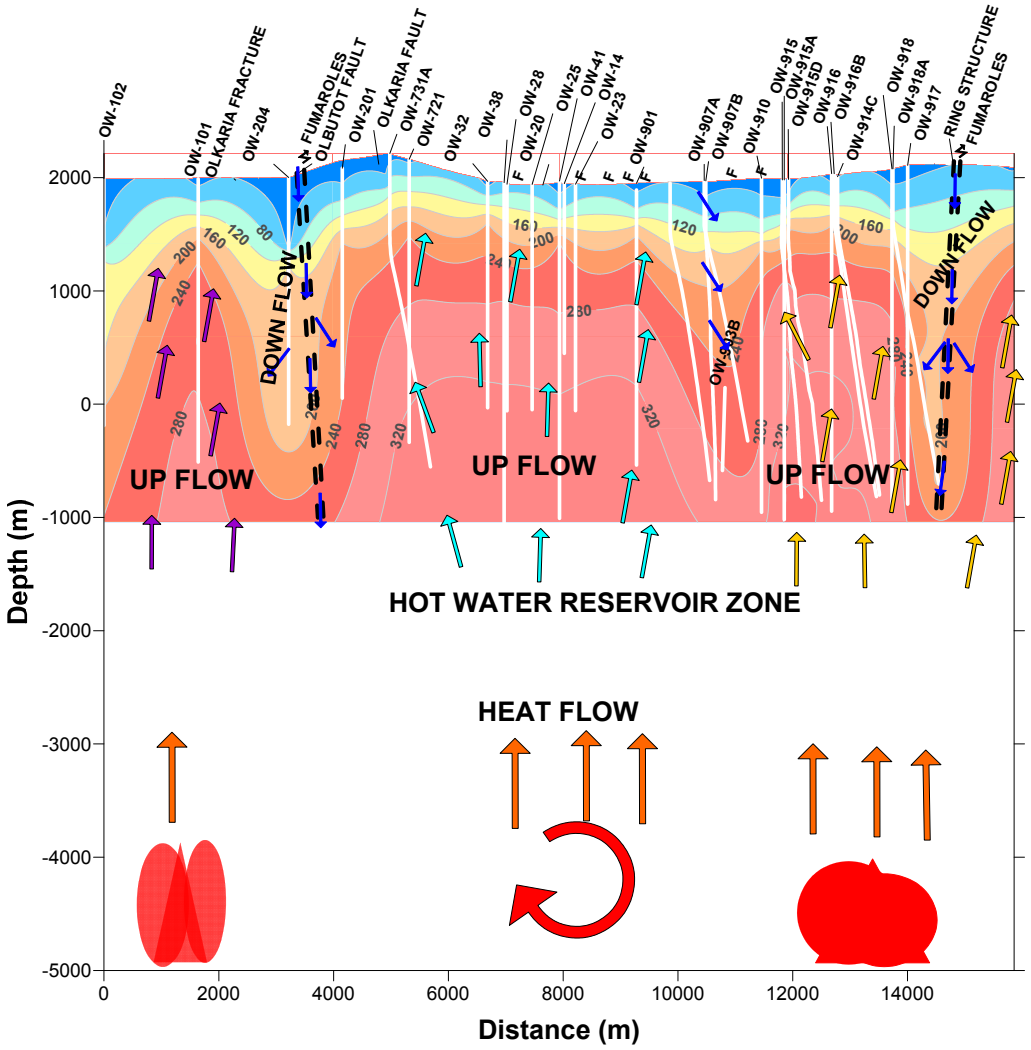

FIGURE 32: Revised conceptual model

Gas geothermometers indicated a temperature of 250°C; surface manifestations such as fumaroles, altered grounds and steaming grounds indicate the likelihood of good permeability.

4. DISCUSSION

Figure 33 shows a map of Olkaria with the structures and location of the newly drilled wells, together with the old wells. Areas with resistivity of interest are also marked, based on the resistivity analysis at -400 m of Olkaria Domes done by Wanjohi in 2011, shown in Figure 6. Also mapped are the centres at 6 km depth to the top of seismic wave attenuating bodies, presented by Mannvit/ ÍSOR/Vatnaskil/Verkís (2011), shown in Figure 5.

The high temperature of 362°C encountered in Well OW-733B at the well's bottom suggests that the well penetrated an up-flow zone near the Gorge farm volcanic centre, believed to be associated with the heat source for the Olkaria Northeast and the Olkaria East production fields. Very high temperatures of close to 381°C were also encountered in Well OW-919A in the Domes field at a depth of 2980 m from the surface. This well was directionally drilled towards the centre of the area, believed to be above the heat source for the Olkaria Domes field.

The horizontal sections confirm the location of four major up-flow zones for the Olkaria field, shown by the pattern of high temperature areas moving from a horizontal section at 1200 to -400 m a.s.l. (Figures 19-25 and Figure 1 in Appendix II).

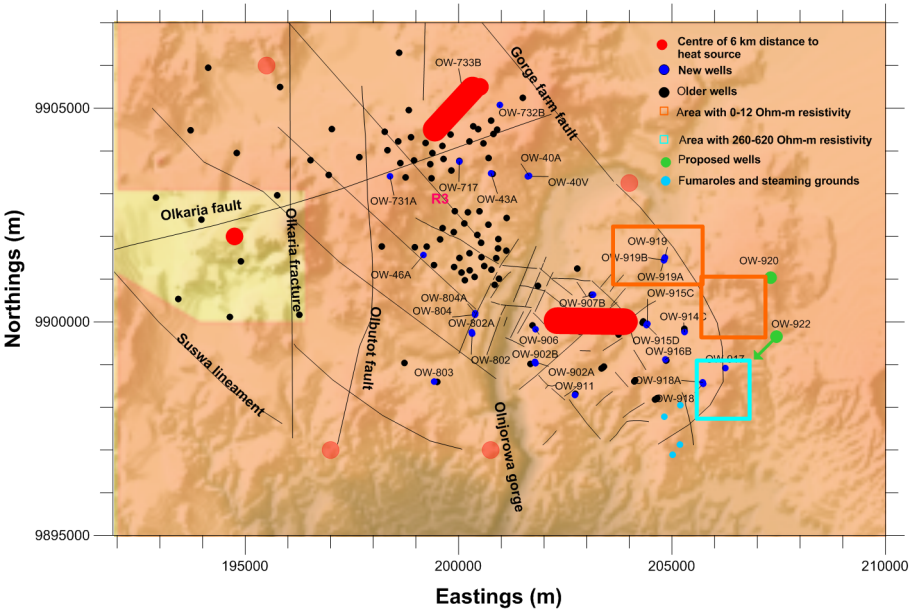

FIGURE 33: Map of the Olkaria geothermal system, showing faults and fractures; main and proposed heat sources and areas mapped from the resistivity

Cooling was witnessed around new Well OW-717 in the NEPF, with a temperature reversal in Wells OW-731A and OW-732B. The temperature reversal in Well OW-731A was confirmed by alteration minerals which indicate a cold inflow and low temperatures. Low enthalpies of 1060 and 1580 kJ/kg were encountered in Wells OW-732B and OW-717 which may further confirm cooling in the region. Temperature reversals may suggest horizontal inflow of colder fluids at upper zones and out flow in the lower formations. This indicates that there could be a fracture taking in cold fluids either from the Ololbutot fault or re-injection Well R3 to these areas. It could also suggest that Well OW-731A is located at the boundary of the colder zone and the East field, separated by the Ololbutot fault. It is worth noting that this cooling was observed along the Olkaria fault as the wells are aligned along this fault.

There is also a possibility of the colder water being re-injected in Well R-3 finding its way through the fracture that is near it, all the way to the Olkaria fault and then eastwards. This could explain the colder zone shown in the 0 m a.s.l. contour map (Figure 23), separating the Northeast production field and the East production field.

The low temperature witnessed in Well OW-40V may confirm that the well is far from any heat source, as shown in Figure 5 and mapped in Figure 33. The heat source near this well, as shown in Figure 5, is deeper than 13 km and may not have strike fractures connected to other up-flow zones. The increase in temperature in Well OW-40A, which was drilled directionally eastwards from the same well pad, may confirm increasing temperatures eastwards near the heat source centre located to the east of Well OW-40V, which is near the Gorge farm fault, shown in Figure 33. It is also important to note that Well OW-40A encountered high down-hole pressures. This could indicate that an exploitable geothermal resource could possibly exist east of the Olkaria Northeast field, due to its proximity to the Gorge farm fault.

Temperature and pressure were observed to increase gradually from Well OW-804 in the Southeast production field to the Domes area, and then suddenly rise as the up flow zone near Well OW-914 was crossed. This explains why the upper and central parts of the Southeast production field had good temperatures. It also shows that the up-flow zone in the Domes field extends to the east and temperature in the newly drilled wells there, Wells OW-914C and OW-914D, showed no evidence of a boundary.

A temperature cross-section from the south to the east showed an up-flow zone, as was expected, in the East production field, then slight cooling around Wells OW-731A and OW-717, followed by an up-flow

zone associated with the Northeast production field. The boundary in the north has not yet been delineated by present drilling and it is possible that the geothermal resource extends northwards.

Well OW-918A, drilled across the southeast corner of the ring structure in the Domes field, showed a temperature reversal at 1700 m from the surface. Well OW-917 drilled near it showed conductive heating to the well bottom and Well OW-918 showed conductive heating to about 1500 m depth, confirming poor permeability in the area penetrated by these wells. The resistivity survey discussed earlier in this section shows a high resistivity anomaly in the range of 260-620 Ωm. This could indicate impermeable rock.

The lithology shows that the dominant rock is trachyte (Musonye, 2013). The temperature reversal witnessed in Well OW-918A suggests a horizontal flow in the vicinity of this well. Low-temperature alteration minerals were encountered, confirming cold water inflow. A temperature regime of cold-hot-cold from an analysis of the alteration minerals and calcite deposition on fractures, also confirmed the horizontal cold flow in this region.

The resistivity of the Olkaria Domes (Figure 6) showed a resistivity of 12-19 Ωm bordering a region of very low resistivity, 0-12 Ωm, in the vicinity of the heat source, as shown in Figure 32, suggesting a potentially good production zone. The high conductivity could be due to water filled fractures with good permeability. Figure 33 illustrates that this region of high conductivity follows the ring structure. The higher resistivity bordering the low resistivity could be due to high-temperature alteration minerals. The southeast part of the Domes field has the same characteristics with the highly conductive region, likely following the outer ring structure. This could imply that the geothermal resource could possibly extend to the southeast and east of Domes field, as earlier suggested. The above discussion explains the conceptual model, as shown in Figure 32, in Section 3.4.

5. CONCLUSIONS

The temperature and pressure model of the Greater Olkaria geothermal field has been updated, based on newly acquired well temperature and pressure data. The resulting additions to the present conceptual model have also been pointed out. It can, therefore, be concluded that:

1. The heat source for the Olkaria geothermal system is, as previous theorized, explained by Mannvit/ÍSOR/Vatnaskil/Verkís who did the field optimisation study shown in Figure 5.
2. Four major up-flow zones have been confirmed, feeding the Olkaria West, Olkaria East, Olkaria Northeast and the Olkaria Domes fields.
3. The geothermal resource extends further north and to the east of the KenGen concession area in Olkaria.
4. Possible resources also exist east of the Northeast field and the southeast part of Domes field.
5. Permeability is believed to be controlled by NW-SE, NE-SW tending faults as well as the ring structure.
6. Cooling of the system was observed around Wells OW-731A, OW-732B and OW-717.
7. Down flow is likely occurring along the ring structure in the southeast part of the Olkaria Domes field, which could possibly be a cold recharge zone. Ololbutot fault has been confirmed as being responsible for the cold water recharge to the field.

Based on the above conclusions, it is further recommended:

1. That a well be sited outside the high-resistivity anomaly experienced near the ring structure in the southeast part of the Domes field and east of Well OW-914C, so as to gain a better understanding

of that area. The proposed Wells OW-922 and OW-920 are located in the region and the study supports the siting of these wells.

2. To consider another area in the northern part of the Northeast production field where indications of a boundary have not yet been encountered.
3. To conduct further investigations to better understand the cooling around Well OW-717 and to explain the origins of the cooling.

ACKNOWLEDGEMENTS

I take this opportunity to sincerely thank the United Nations University Geothermal Training Programme and the Government of Iceland for granting me an opportunity to improve my skills in geothermal energy development. Special thanks go to the outgoing director of the UNU-GTP, Dr. Ingvar B. Fridleifsson, the present director Mr. Lúdvík S. Georgsson, Ms. Thórhildur Ísberg, Mr. Ingimar G. Haraldsson, Mr. Markús A. G. Wilde, and Ms. Málfrídur Ómarsdóttir for their assistance throughout the course. I extend my gratitude to my supervisors, Ms. Saeunn Halldórsdóttir, Ms. Sigrídur Sif Gylfadóttir from ÍSOR and Mr. Andri Arnaldsson. Special thanks to all other ÍSOR staff, especially Dr. Gudni Axelsson and Mr. Benedikt Steingrímsson, for guidance and their valuable time in reviewing my project report together with Mr. Benedikt Steingrímsson, for guidance and their valuable time in reviewing my project report.

I am indebted to Kenya Electricity Generating Company (KenGen) management for granting me leave to attend this informative course and for allowing me use of the company's data for my project. I also thank my colleagues in the company for their assistance in the provision of good data for my project. I say thank you to the 2013 UNU Fellows for their company and fruitful discussions during my stay in Iceland. I would also like to take this opportunity to thank my family and wife for giving me moral support, love, prayers and encouragement.

Finally, I want to thank God for the good health, strength and his blessings during my stay in Iceland.

REFERENCES

Arason, T., Björnsson, G., Axelsson, G., Bjarnason, J.Ö., and Helgason, P., 2004: *ICEBOX – geothermal reservoir engineering software for Windows. A user's manual.* ISOR, Reykjavík, report 2004/014, 80 pp.

Axelsson, G., Arnaldsson, A., Gylfadóttir, S.S., Halldórsdóttir, S., Mortensen, A.K., Bore, C., Karingithi, C., Koech, V., Mbithi, U., Muchemi, G., Mwarania, F., Opondo, K., and Ouma, P., 2013: Conceptual model and resource assessment for the Olkaria geothermal system, Kenya. *Proceedings of the "Short Course V on Conceptual Modeling of Geothermal Systems", organized by UNU-GTP and LaGeo, Santa Tecla, El Salvador*, 21 pp.

Barelli, A., and Palama, A., 1981: New method for evaluating formation equilibrium in holes during drilling. *Geothermics, 10-2,* 95-102.

Clarke, M.C.G., Woodhall, D.G., Allen, D., and Darling G., 1990: *Geological, volcanological and hydrogeological controls on the occurrence of geothermal activity in the area surrounding Lake Naivasha, Kenya, with coloured 1:100 000 geological maps.* Ministry of Energy, Nairobi, 138 pp.

Dowdle, W.L., and Cobb, W.M., 1975: Static formation temperature from logs - an empirical method. *J. Petroleum Technology, 27-11*, 1326-1330.

Grant, M.A., and Bixley, P.F., 2011: *Geothermal reservoir engineering, 2nd edition*. Academic Press, New York, 359 pp.

Grant, M.A., Donaldson, I.G., and Bixley, P.F., 1982: *Geothermal reservoir engineering*. Academic Press, New York, 369 pp.

Mannvit/ÍSOR/Vatnaskil/Verkís Consortium, 2011: Revision of the conceptual model of the Greater Olkaria Geothermal System-Phase I. Mannvit/ÍSOR/Vatnaskil/Verkís, Reykjavík, 100pp.

Mannvit/ÍSOR/Vatnaskil/Verkís Consortium, 2012a: Volumetric resource assessment and lumped parameter pressure response modelling of the Greater Olkaria Geothermal System-Phase I. Mannvit/ISOR/Vatnaskil/Verkís, Reykjavík, March, 43pp.

Mannvit/ÍSOR/Vatnaskil/Verkís Consortium, 2012b: Development of the numerical model of the Greater Olkaria Geothermal System-Phase I. Mannvit/ÍSOR/Vatnaskil/Verkís, Reykjavík, June, 111pp.

Mariita, N.O., 2009: Exploration history of Olkaria geothermal field by use of geophysics. *Paper presented at "Short course IV on exploration for geothermal resources", UNU-GTP, KenGen and GDC, Lake Naivasha, Kenya*, 13 pp.

Muchemi, G.G., 1999: *Conceptualised model of the Olkaria geothermal field.* The Kenya Electricity Generating Company, Ltd., internal report, 46 pp.

Mungania, J., 1992: *Geology of the Olkaria geothermal complex.* Kenya Power Company, Ltd., internal report, 38 pp.

Mungania, J., 1999: *Summary of updates of the geology of the Olkaria Domes geothermal field.* Kenya Electricity Generating Company, Ltd., unpublished report.

Musonye, X.S., 2013: *Borehole geology and alteration mineralogy of well OW-917, Domes area, Olkaria geothermal field, central Kenya rift.* The Kenya Electricity Generating Company, Ltd., internal report, 33 pp.

Naylor, W.I., 1972: *Geology of the Eburru and Olkaria prospects.* U.N. Geothermal Exploration Project, report.

Ndombi, J.M., 1981: The structure of shallow earth beneath the Olkaria Geothermal field, Kenya, deduced from gravity studies. *J. Volcanol. & Geothermal Research, 9,* 237-251.

Ofwona, C.O., 2002: *A reservoir study of Olkaria East geothermal system, Kenya*. University of Iceland, M.Sc. thesis, UNU-GTP, Iceland, report 1, 74 pp.

Onacha, S.A., Shalev, E., Malin, P., and Leary, P., 2009: *Joint geophysical imaging of fluid-filled fracture zones in geothermal fields in the Kenya Rift valley.* Auckland University, Institute of Earth Science and Engineering, NZ, 6 pp.

Roux, B., Sanyal, S.K., and Brown, S.L., 1980: An improved approach to estimating the reservoir temperature from transient temperature data. *Paper presented at 50th Annual Regional Meeting of the Society of Petroleum Engineers of AIME, Los Angeles,* 5 pp.

Simiyu, S.M., and Malin, P.E., 2000: A "volcano-seismic" approach to geothermal exploration and reservoir monitoring: Olkaria, Kenya and Casa Diablo, USA. *Proceedings of the World Geothermal Congress 2000, Kyushu-Tohoku, Japan,* 1759-1763.

Simiyu, S.M., Oduong, E.O., and Mboya, T.K., 1998a: *Shear wave attenuating beneath the Olkaria volcanic field.* The Kenya Electricity Generating Company, Ltd., internal report, 30 pp.

Stefánsson, V., and Steingrímsson, B.S., 1990: *Geothermal logging I, an introduction to techniques and interpretation* (3rd ed.). Orkustofnun, Reykjavík, report OS-80017/JHD-09, 117 pp.

Sweco and Virkir, 1976: *Feasibility report for the Olkaria geothermal project*. Sweco and Virkir, report prepared for United Nations and Government of Kenya.

Wanjohi, A., 2011: *Geophysics report, east of Olkaria Domes (Akira) geothermal field.* The Kenya Electricity Generating Company Ltd, internal report, 34 pp.

West-JEC, 2009: *The Olkaria optimisation study (phase II) – final reservoir analysis report*. West Japan Engineering Consultants, Inc., 301pp.

APPENDIX I: Temperature and pressure profiles with formation temperatures in recently drilled wells in Olkaria

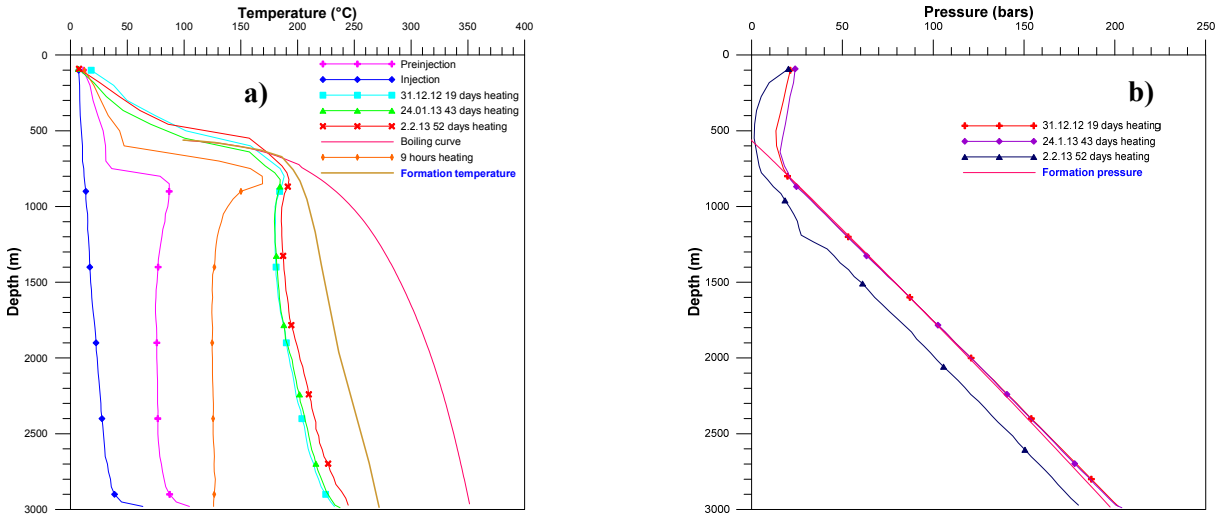

FIGURE 1: Well OW-717: a) Temperature profiles; b) Pressure profiles

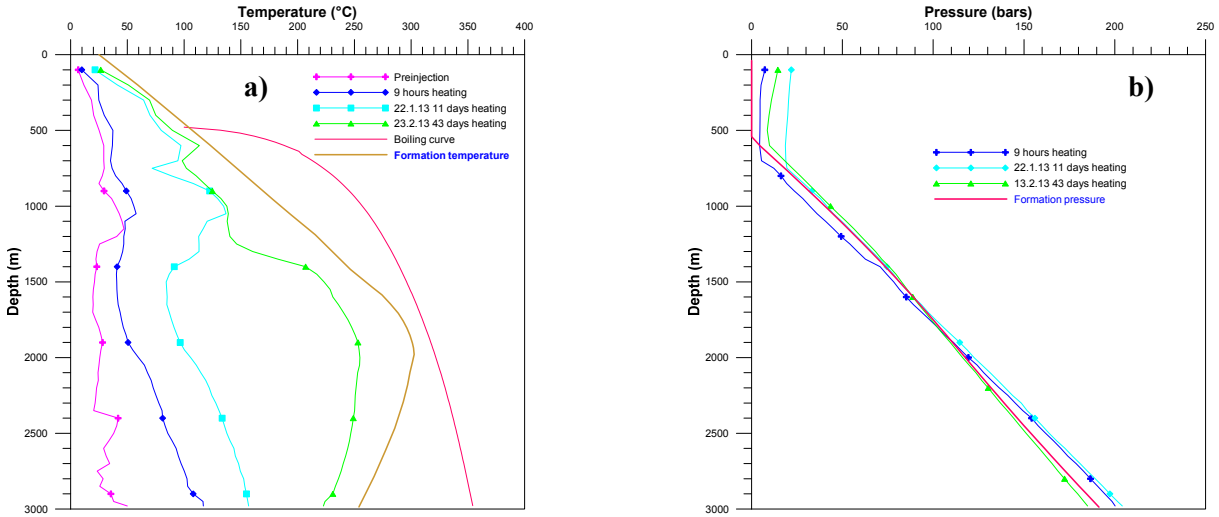

FIGURE 2: Well OW-732B: a) Temperature profiles; b) Pressure profiles

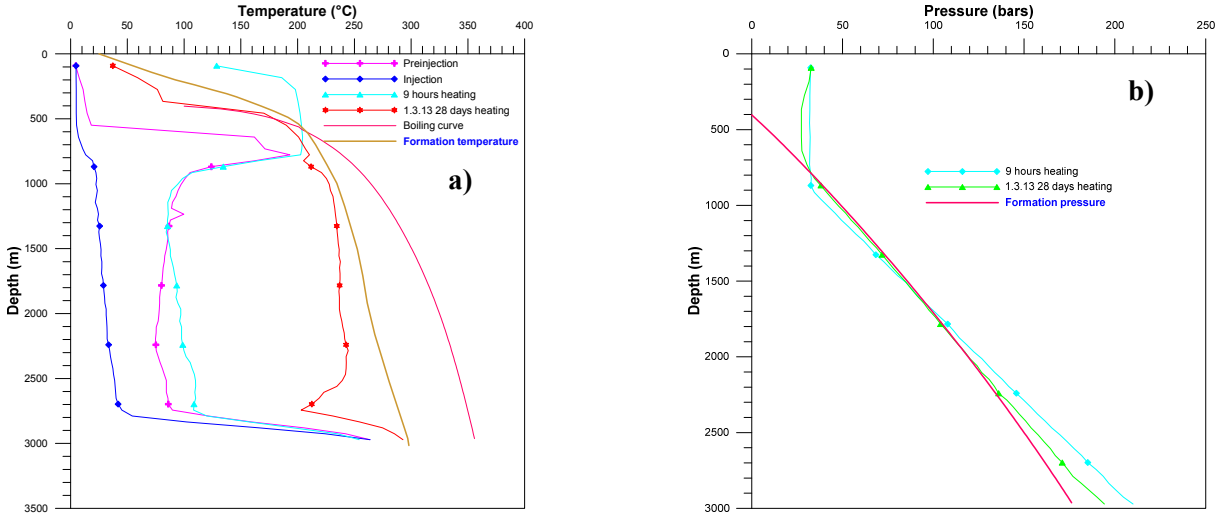

FIGURE 3: Well OW-43A: a) Temperature profiles; b) Pressure profiles

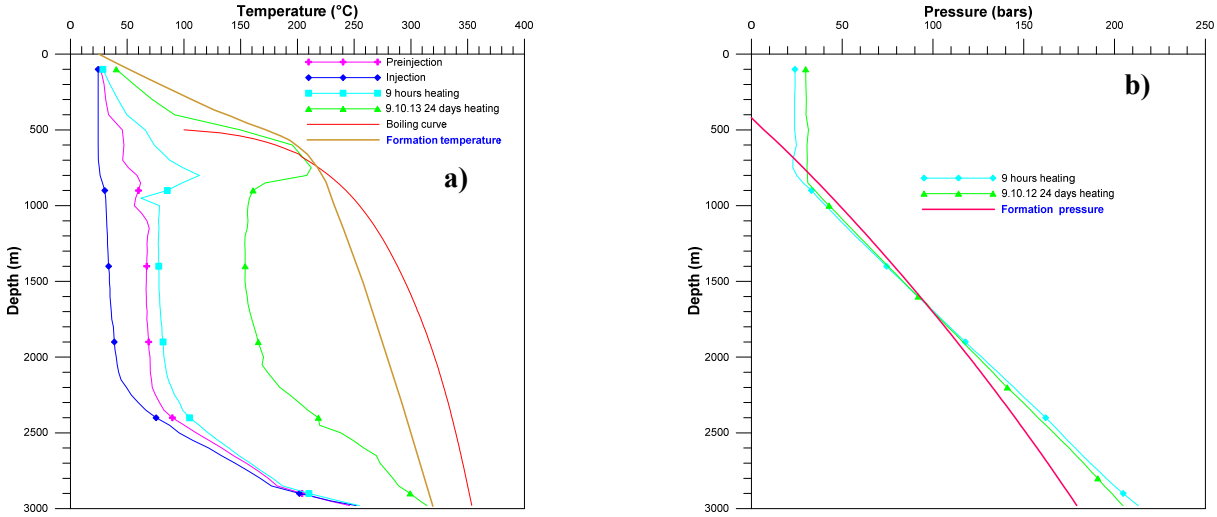

FIGURE 4: Well OW-46A: a) Temperature profiles; b) Pressure profiles

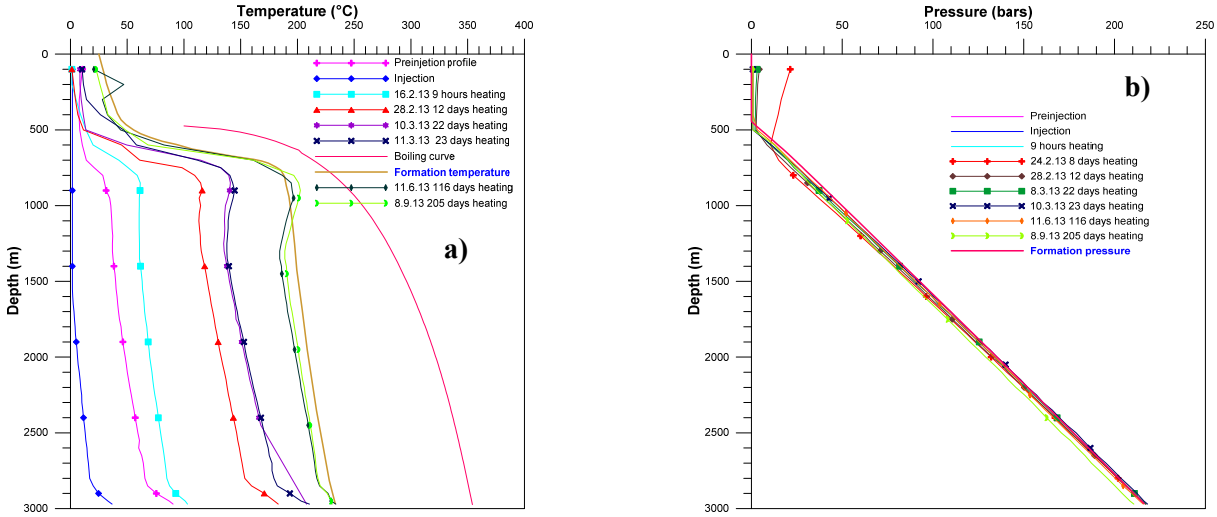

FIGURE 5: Well OW-40V: a) Temperature profiles; b) Pressure profiles

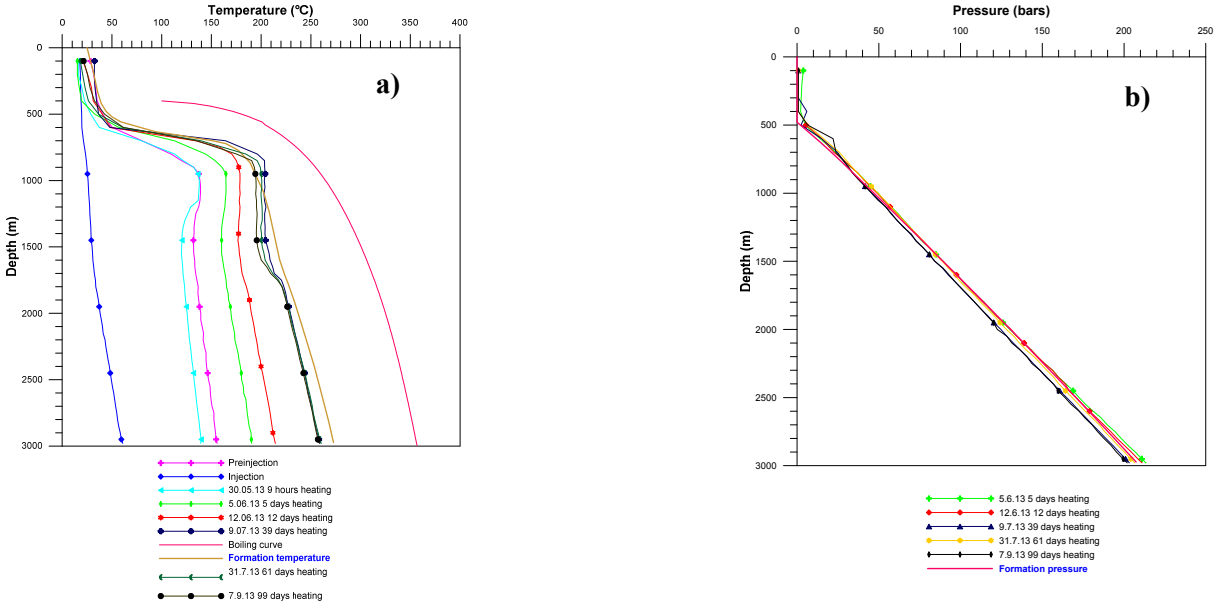

FIGURE 6: Well OW-40A: a) Temperature profiles; b) Pressure profiles

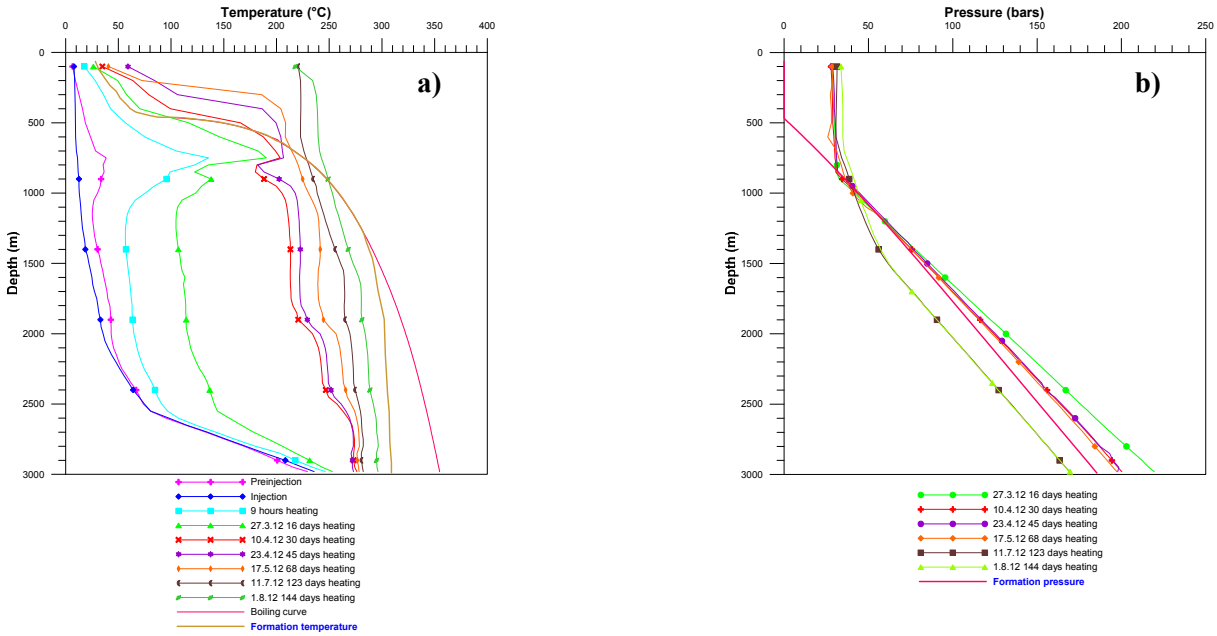

FIGURE 7: Well OW-802: a) Temperature profiles; b) Pressure profiles

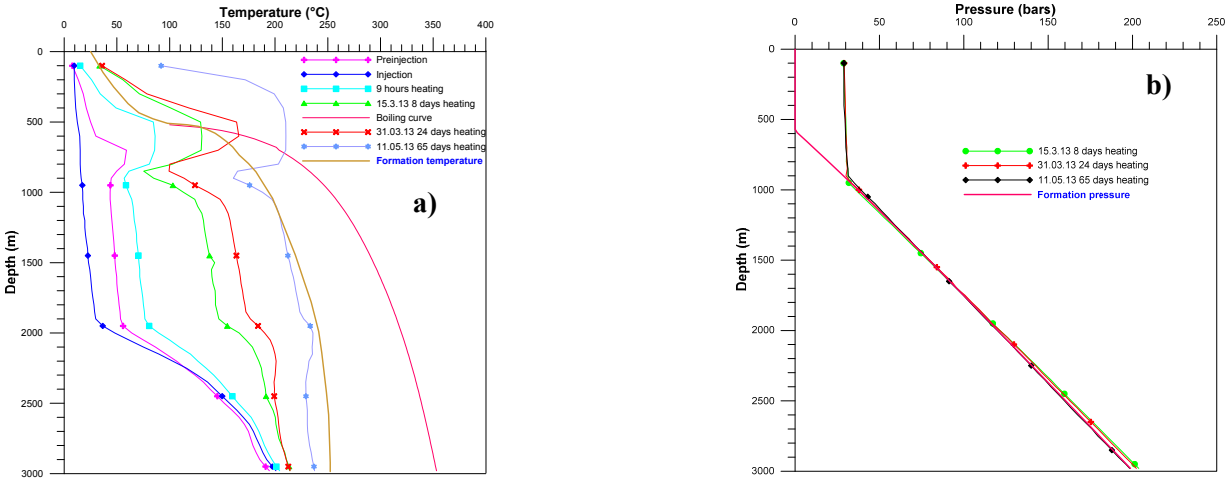

FIGURE 8: Well OW-802A: a) Temperature profiles; b) Pressure profiles

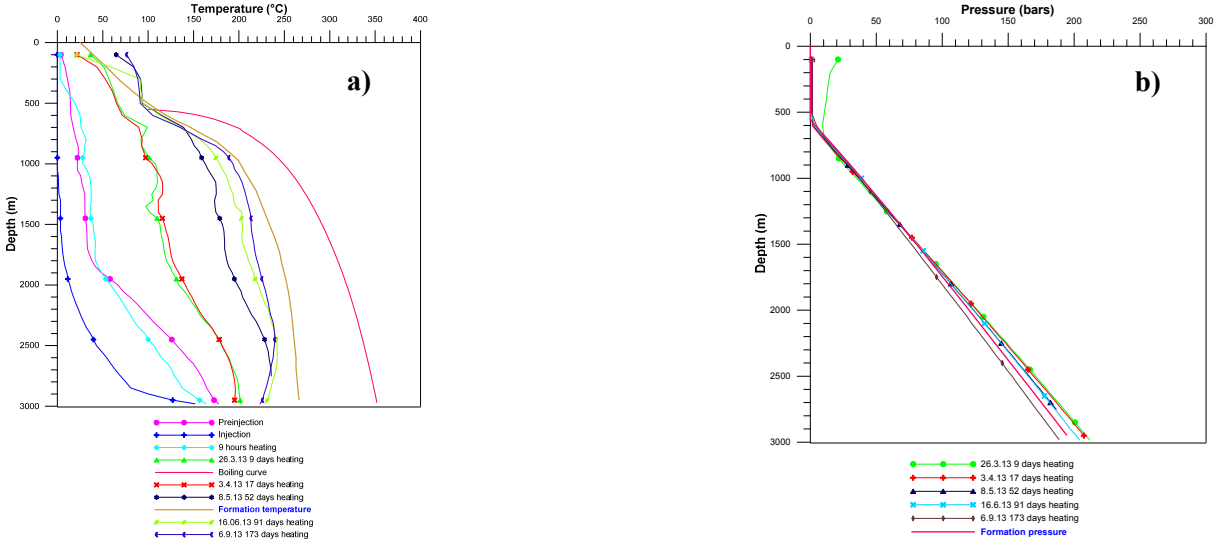

FIGURE 9: Well OW-803: a) Temperature profiles; b) Pressure profiles

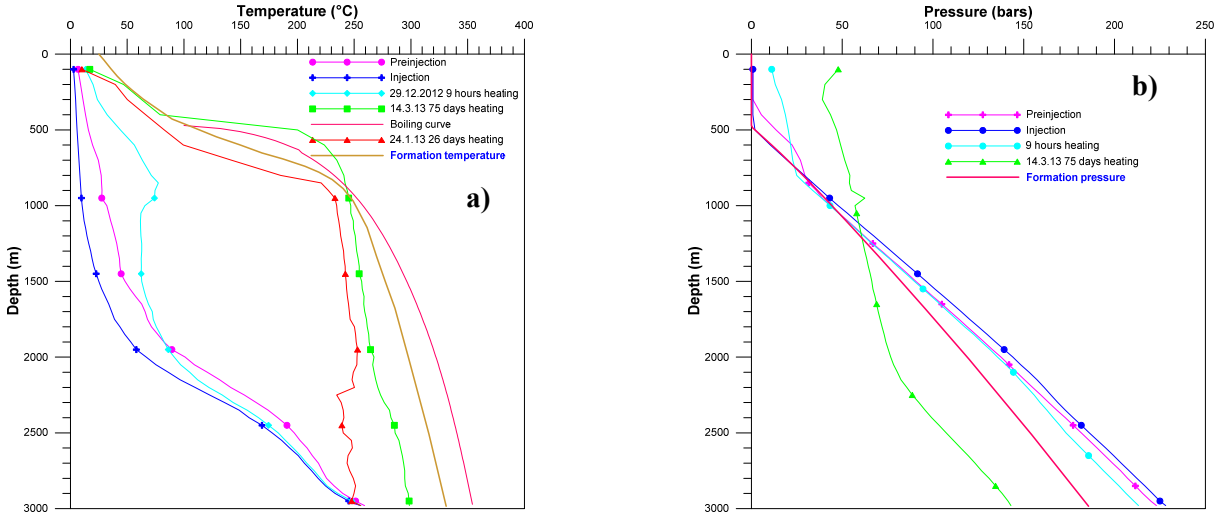

FIGURE 10: Well OW-804: a) Temperature profiles; b) Pressure profiles

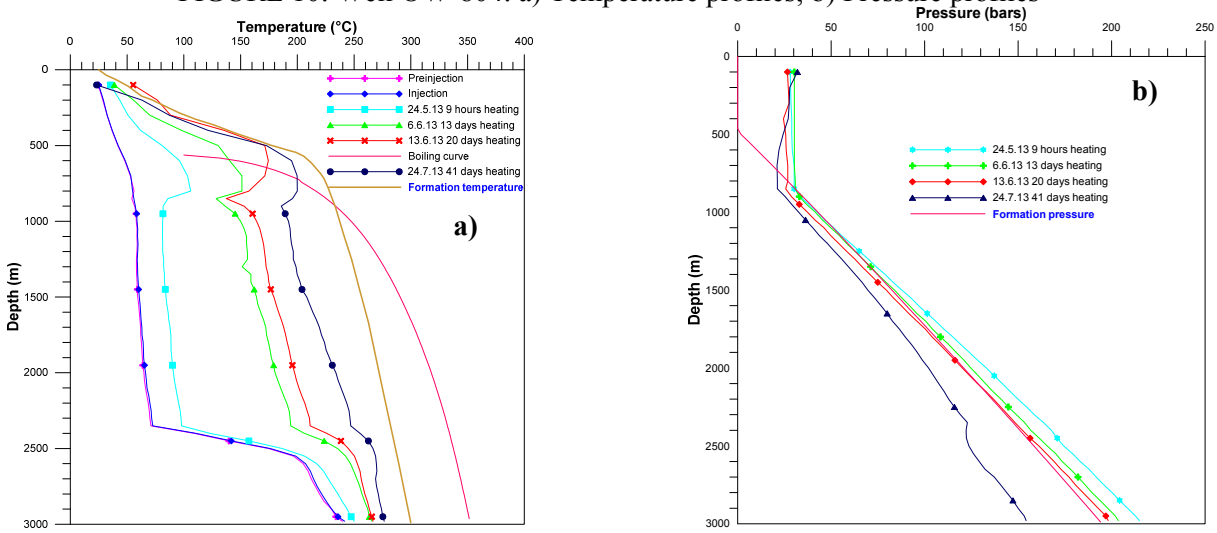

FIGURE 11: Well OW-804A: a) Temperature profiles; b) Pressure profiles

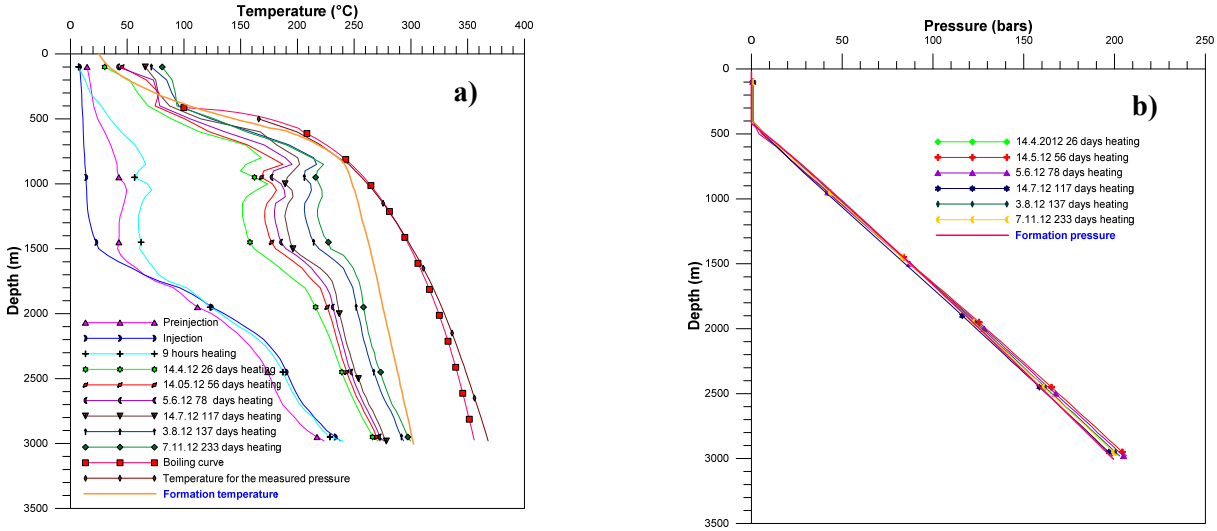

FIGURE 12: Well OW-902A: a) Temperature profiles; b) Pressure profiles

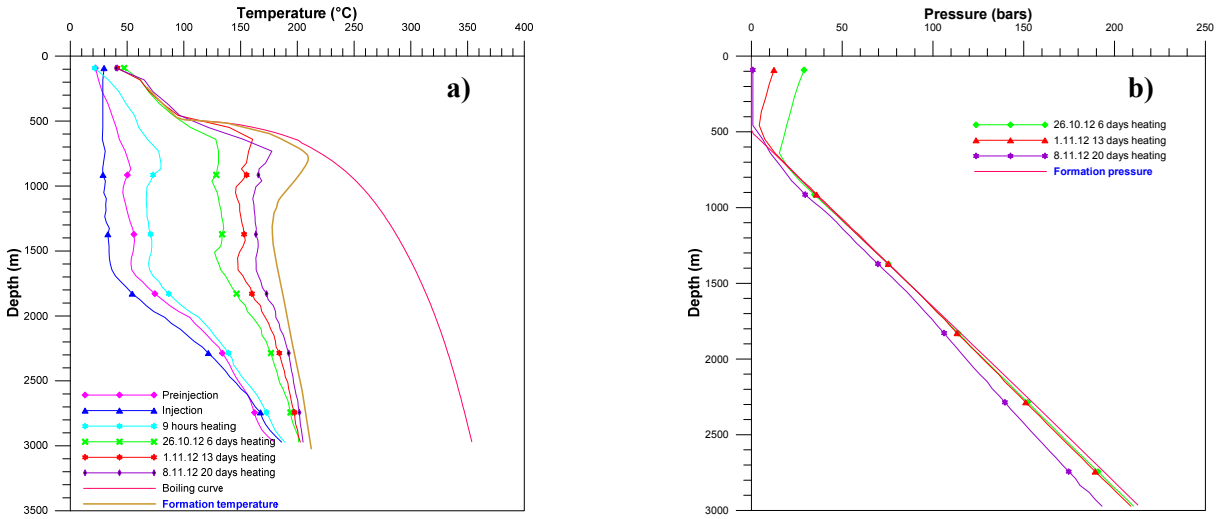

FIGURE 13: Well OW-902B: a) Temperature profiles; b) Pressure profiles

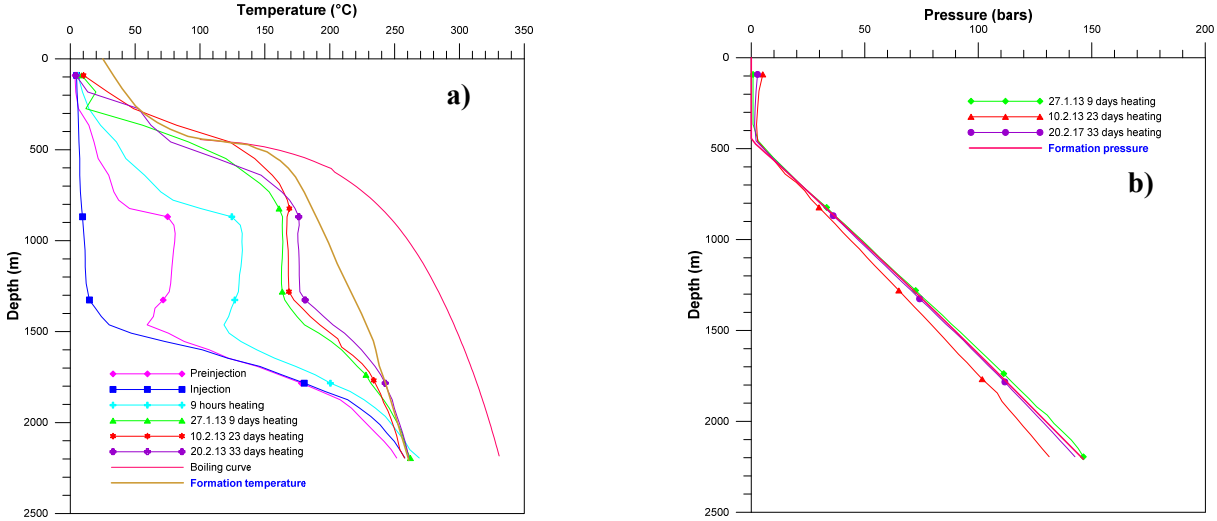

FIGURE 14: Well OW-906: a) Temperature profiles; b) Pressure profiles

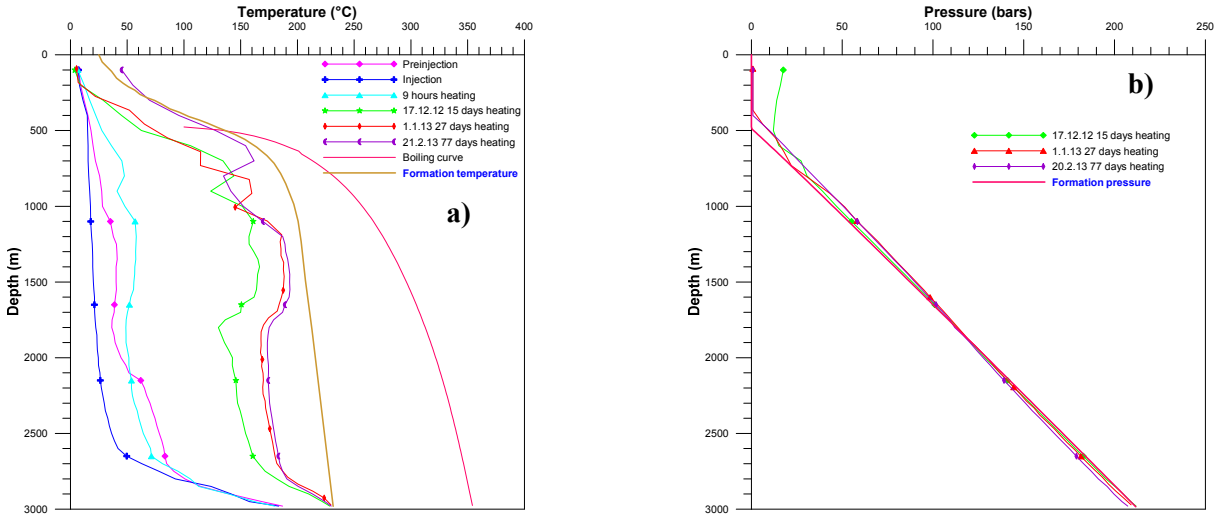

FIGURE 15: Well OW-907B: a) Temperature profiles; b) Pressure profiles

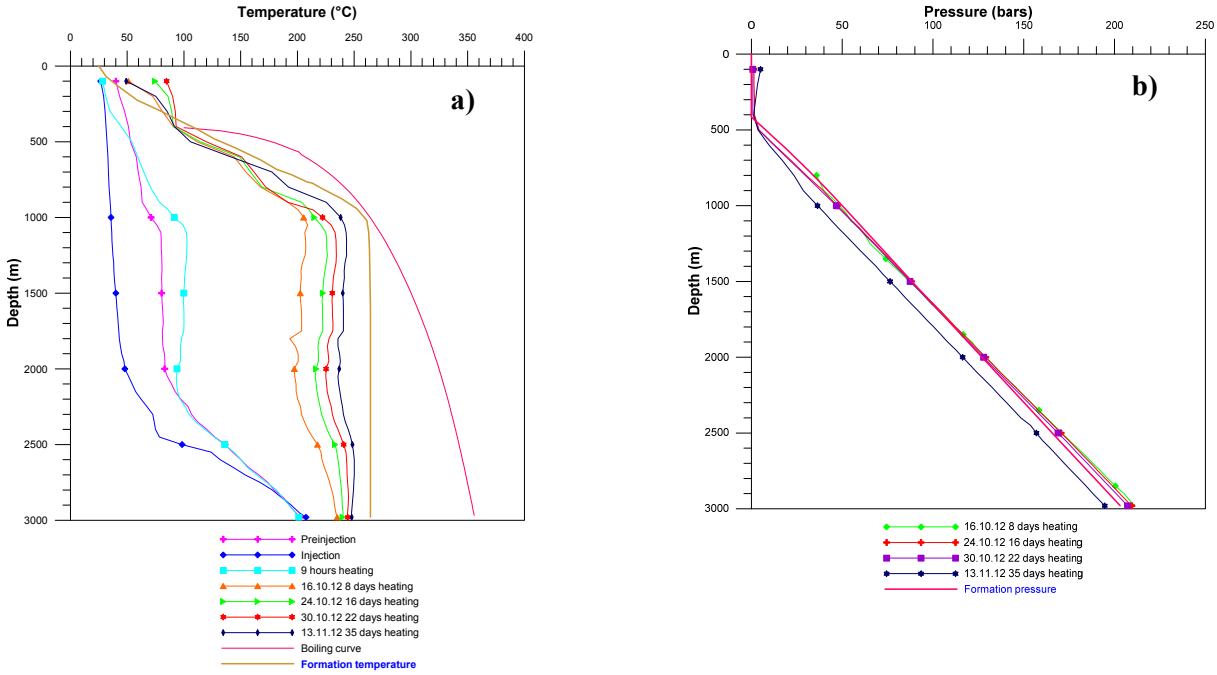

FIGURE 16: Well OW-911: a) Temperature profiles; b) Pressure profiles

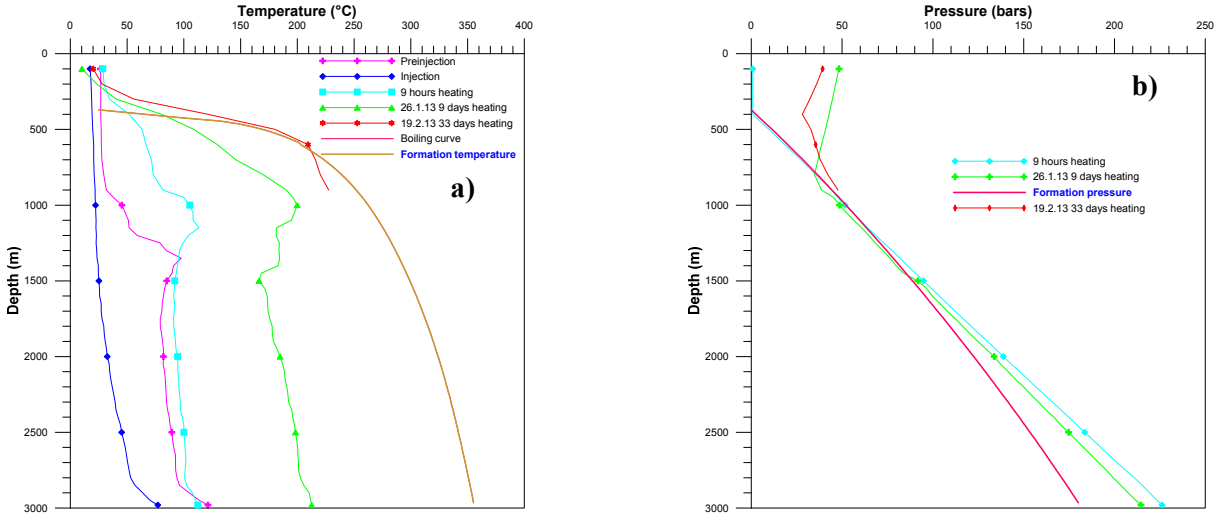

FIGURE 17: Well OW-914C: a) Temperature profiles; b) Pressure profiles

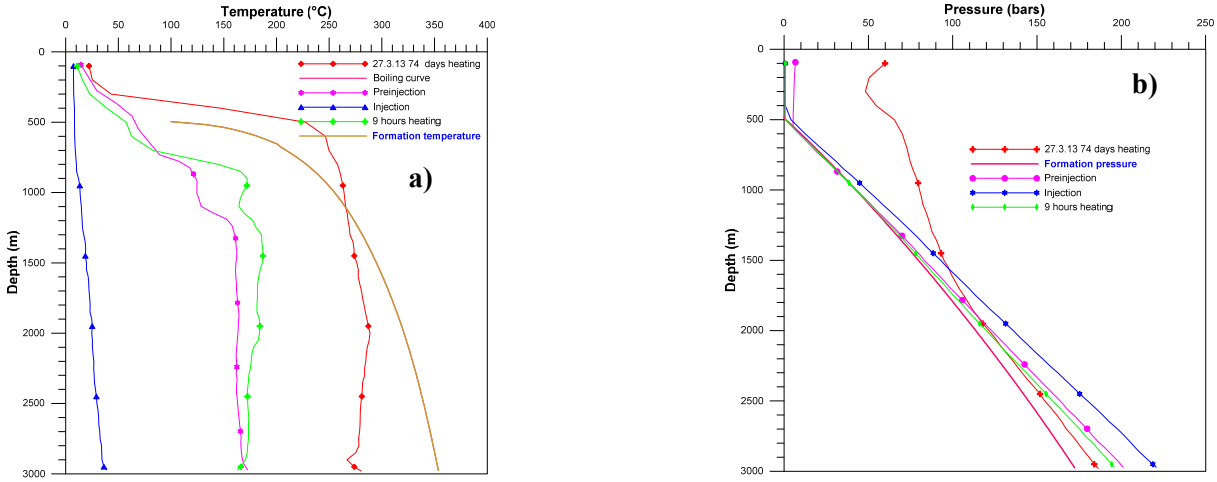

FIGURE 18: Well OW-915C: a) Temperature profiles; b) Pressure profiles

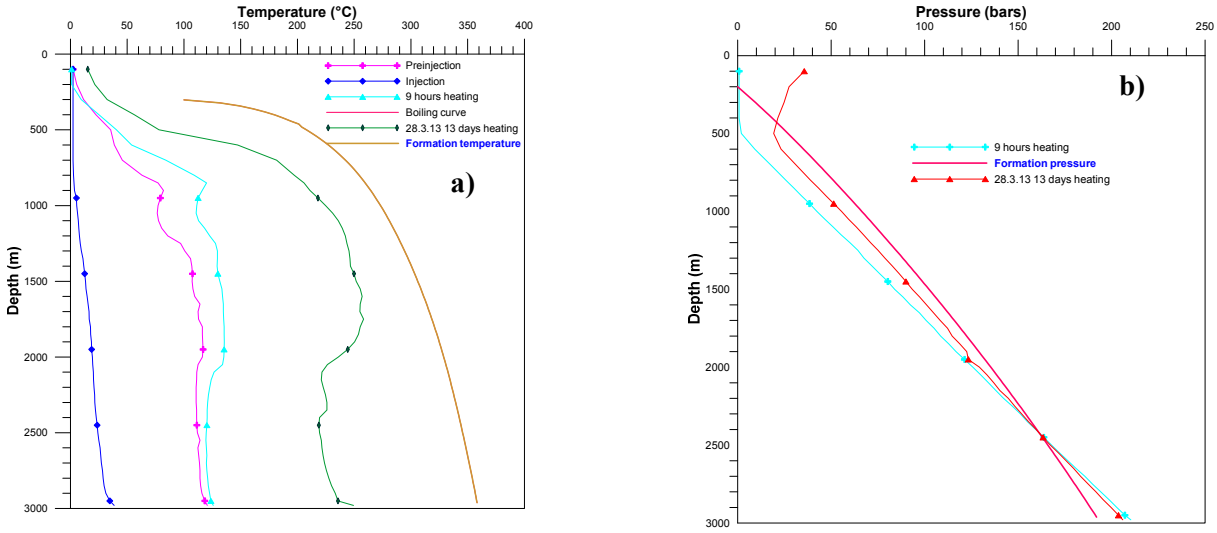

FIGURE 19: Well OW-915D: a) Temperature profiles; b) Pressure profiles

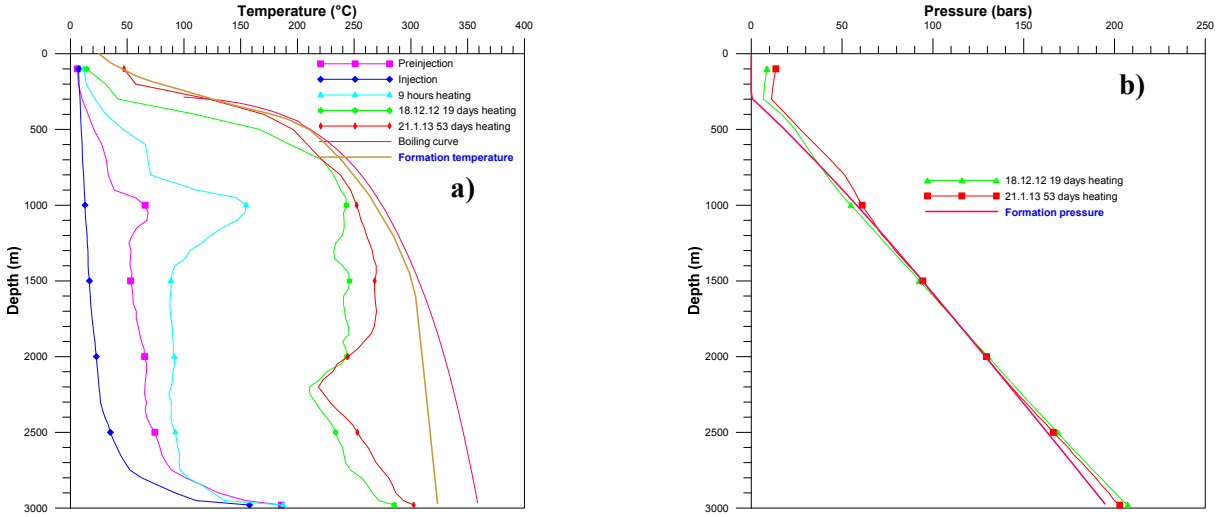

FIGURE 20: Well OW-916B: a) Temperature profiles; b) Pressure profiles

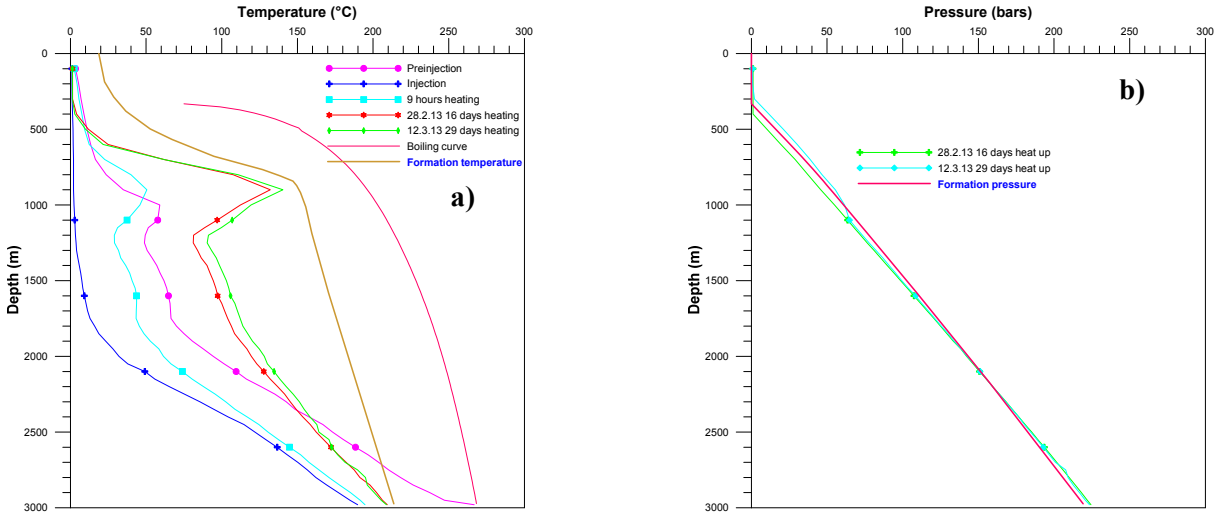

FIGURE 21: Well OW-919: a) Temperature profiles; b) Pressure profiles

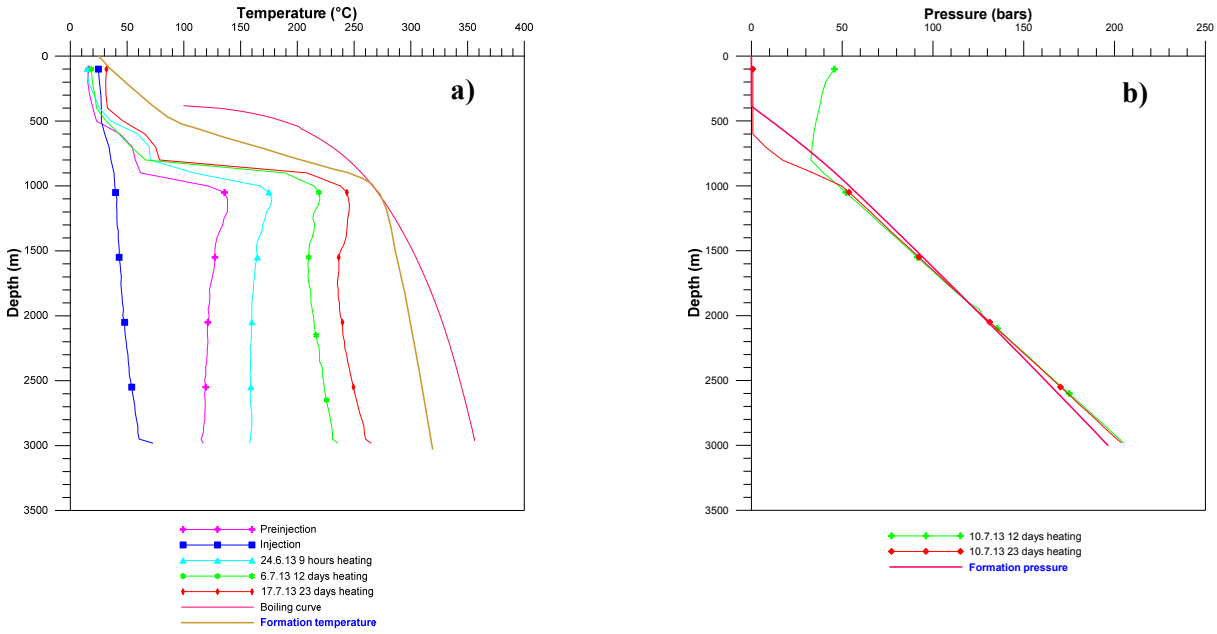

FIGURE 22: Well OW-919B: a) Temperature profiles; b) Pressure profiles

APPENDIX II: Temperature and pressure contour maps for Olkaria at 1200 m a.s.l.

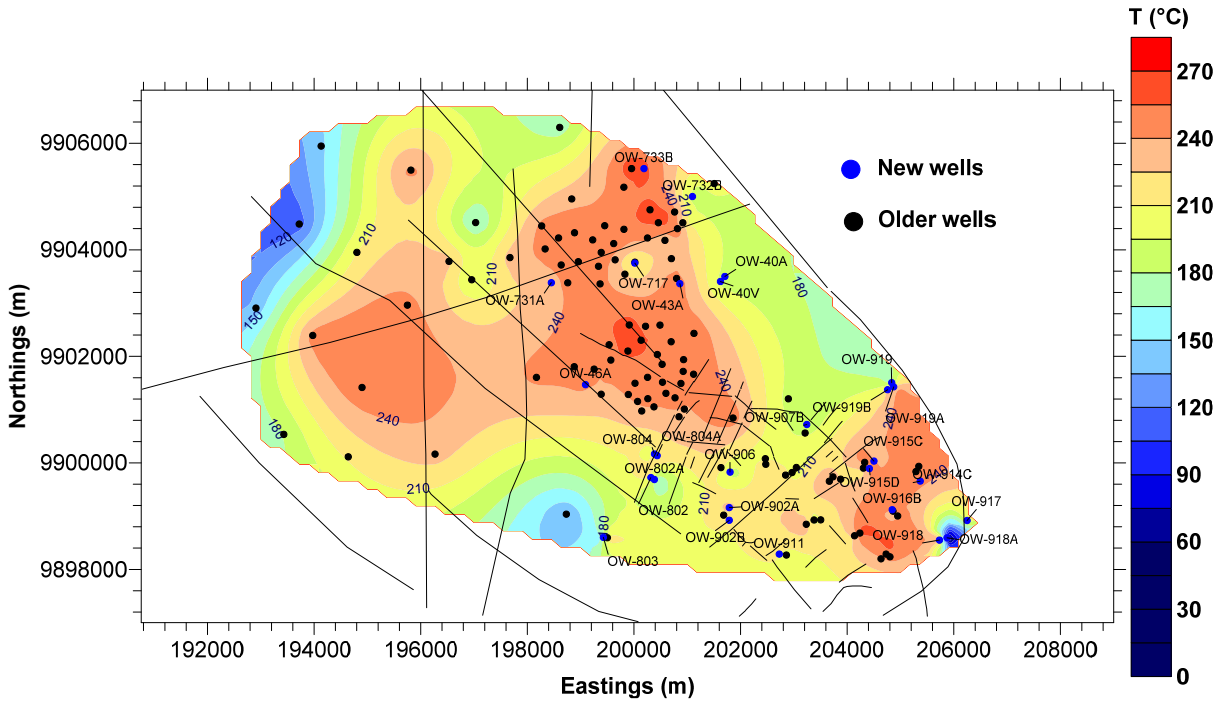

FIGURE 1: Temperature distribution at 1200 m a.s.l.

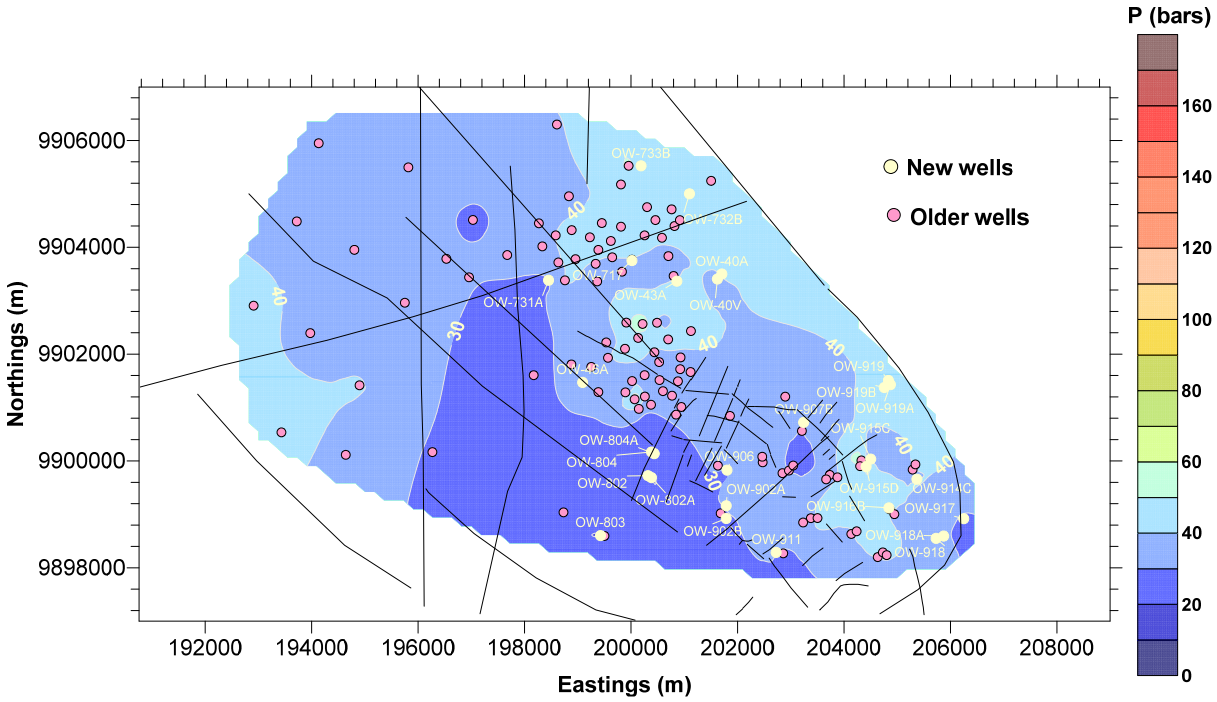

FIGURE 2: Pressure distribution at 1200 m a.s.l.